NOVA SCHOOL OF SCIENCE & TECHNOLOGY

DEPARTMENT OF MATERIALS SCIENCE

JOANA MIRANDA SALREU MARTINHO

Bachelor in Micro and Nanotechnologies Engineering

ENGINEERING AND CHARACTERIZATION OF NOVEL DENATURING PLATFORMS FOR AUTOMATED RELEASE OF miRNAS FROM CARRIER PROTEINS AND EXOSOMES

MASTERS IN MICRO AND NANOTECHNOLOGIES ENGINEERING

NOVA University Lisbon

November, 2022

NOVA SCHOOL OF SCIENCE & TECHNOLOGY

DEPARTMENT OF MATERIALS SCIENCE

ENGINEERING AND CHARACTERIZATION OF NOVEL DENATURING PLATFORMS FOR AUTOMATED RELEASE OF miRNAS FROM CARRIER PROTEINS AND EXOSOMES

JOANA MIRANDA SALREU MARTINHO
Bachelor in Micro and Nanotechnologies Engineering

Adviser: Dr Sylvain Ladame, Reader in Biosensor Development, Imperial College London

Co-adviser: Dr José Ricardo Ramos Franco Tavares, Associate Professor with Aggregation, NOVA University Lisbon

Examination Commitee:

Chair: Dr João Paulo Miranda Ribeiro Borges, Professor with Aggregation, NOVA University Lisbon

Repporteurs: Dr Nuria Oliva-Jorge, Research Fellow, Imperial College London

Members: Dr Sylvain Ladame, Reader in Biosensor Development, Imperial College London

Dr José Ricardo Ramos Franco Tavares, Associate Professor with Aggregation, NOVA University Lisbon

MASTERS IN MICRO AND NANOTECHNOLOGIES ENGINEERING

NOVA University Lisbon
November, 2022

Engineering and characterization of novel denaturing platforms for automated release of miRNA from carrier proteins and exosomes

“I always do that, get into something and see how far I can go.”
(Richard Feynman)

ACKNOWLEDGEMENT

I wish to express my thanks to all those who have in any way allowed this project to come true.

A big and sincerely thank you to my advisor Dr Sylvain Ladame, from Imperial College London, for allowing me to work on his group and for giving me the opportunity and resources to work in this emergent area, as well as all the support, patience, knowledge and guidance.

I would also like to thank my co-advisor Dr José Ricardo Ramos Franco Tavares, from NOVA School of Science and Technology, for all the insightful conversations and suggestions that always had a practical outcome.

To Imperial College London, thank you for accepting me during this short period and for providing such great research facilities that allow for scientific knowledge to thrive.

To all the amazing people that I have met and were part of my stay at ICL, in London, thank you so much for all the great and fun moments, and for always pushing me to challenge myself. Without you guys it would have been way more tedious.

To the NOVA School of Science and Technology, thank you for being my second home during the past six years, for the excellence and the amazing campus.

To the Materials Science Department (DCM) for the opportunity, quality teaching and excellent relation established between teachers, researchers and students.

To Dr Rodrigo Martins and Dr Elvira Fortunato for creating an academic path in Portugal highly focused on future technologies, providing all the facilities available for students' development.

Aos meus pais, Cristina e Emanuel (ou Emanuel e Cristina, não quero criar favoritismos), que sempre me apoiaram e cultivaram os meus horizontes. Se cheguei onde cheguei hoje é porque me apoiaram, educaram e estiveram presentes em todas as etapas importantes da minha vida.

À minha irmã, Mafalda, que foi a minha primeira amiga no mundo e que com o tempo ainda se torna mais. Obrigada por testares a minha paciência, conduziu-me à pessoa que sou hoje. Mas mais que tudo, por estares sempre disponível para me ajudar e dar bons conselhos.

Aos meus avós, a quem eu durante seis anos tive de explicar o que era o meu curso, um obrigada por sempre se preocuparem comigo e por contribuírem para a minha educação. Os valores que hoje levo comigo em muito se devem à vossa presença na minha vida.

Por fim, ao último membro do agregado familiar, a minha cadela Maré que está sempre feliz por me ver e que sempre foi a minha companheira de corridas e passeios, mas também quando preciso de ânimo.

À minha amiga Mafalda, que sempre me acompanhou desde que tinha 6 anos. Obrigada por todas as brincadeiras, conselhos e desabafos que tivemos ao longo dos anos.

Aos meus amigos da Ericeira, obrigada por tornarem os meus fins de semana uma alegria, por sempre estarem lá para mim quando necessitei e por todas as aventuras que já tivemos.

Aos meus amigos da faculdade, em especial à Mariana, muito obrigada por terem feito parte da minha vida nestes últimos anos. Adorei todas as nossas conversas parvas, brincadeiras e convívios.

A todos vocês, muito obrigada!

RESUMO

A transição de miRNAs provenientes de biópsias líquidas em biomarcadores para dispositivos de point-of-care (POC) tem sido limitada devido aos passos de pré-processamento necessários para a análise de amostras. A ambiguidade na literatura relativamente à sua biogénese prejudica a deteção e standardização dos protocolos de extração de miRNAs.

Aqui, moléculas derivadas de guanidina foram produzidas para agir como poderosos agentes denaturantes, permitindo a libertação de miRNAs dos portadores. Estas moléculas foram então acopoladas a hidrogéis e a partículas magnéticas, permitindo a construção de dois mecanismos de extração de miRNA diferentes. As matrizes de hidrogéis funcionalizadas desnaturaram com sucesso as proteínas e enalteceram as propriedades desnaturantes das moléculas de guanidina acopladas, devido à estrutura tridimensional intrínseca. Da mesma forma, o mecanismo de desnaturação composto por partículas magnéticas induziu a desnaturação de proteínas e foi ainda testado para a libertação de miRNA a partir de amostras de plasma. Este método de extração exigiu menos etapas de processamento e reduziu a utilização de reagentes tóxicos. O qPCR foi utilizado para quantificar a concentração de miR-21 após a extração, mostrando que foram extraídas baixas concentrações deste miRNA com a utilização dos MBs.

Os sistemas de desnaturação aqui estudados podem ajudar a contribuir para a standardização da extração de miRNA, assim como incentivar novos dispositivos POC com libertação de miRNA on-chip, promovendo a utilização de miRNAs provinientes de biópsias líquidas como biomarcadores.

Palavras-chave: agentes desnaturantes, dispositivos de POC, extração de miRNA, hidrogéis, standardização, partículas magnéticas, qPCR.

ABSTRACT

Translation of miRNAs from liquid biopsies into biomarkers for point-of-care (POC) devices has been limited due to the pre-processing steps needed for sample analysis. The ambiguity in literature regarding its biogenesis impairs miRNA detection and standardization of extraction protocols.

Herein, guanidine derived molecules were produced to act as powerful denaturing agents, enabling miRNA release from carriers. This molecules were then coupled to hydrogels and magnetic beads (MBs), allowing to construct two different miRNA extraction mechanisms. The functionalized hydrogel matrixes successfully unfolded proteins and enhanced the denaturing properties of the coupled guanidine molecules, due to their intrinsic three-dimensional network. Similarly, the MBs denaturing mechanism induced protein unfolding and it was further tested for miRNA release from plasma samples. This extraction method required less processing steps and reduced the usage of toxic reagents. The qPCR was used to quantify the miR-21 concentration post extraction, showing that low quantities of this miRNA were extracted when using the MBs.

The denaturing systems here studied can help contribute towards the standardization of miRNA extraction was well as encourage new POC devices with on-chip miRNA release, to further promote the use of miRNAs from liquid biopsies as biomarkers.

Keywords: denaturing agents, hydrogels, magnetic beads, miRNA extraction, POC devices, qPCR, standardization.

TABLE OF CONTENTS

ACKNOWLEDGEMENT ..... **IX**

RESUMO ..... **XII**

ABSTRACT ..... **XIV**

TABLE OF CONTENTS ..... **XVI**

LIST OF FIGURES ..... **XIX**

SYMBOLS ..... **XXII**

ACRONYMS ..... **XXIV**

1. MOTIVATION AND OBJECTIVES **26**

2. INTRODUCTION **28**

2.1. miRNAs as Biomarkers 28
2.2. miRNA Isolation 29
2.3. Protein Denaturation - Guanidine Derivatives 29
2.4. Denaturing Platforms 30
2.4.1. Hydrogel *30*
2.4.2. Magnetic Beads *30*
2.5. Project Aims 31

3. MATERIALS AND METHODS **34**

3.1. Materials 34
3.2. Synthesis and Characterization of Guanidine Derivatives 34
3.2.1. Guanidinoethyl disulfide Synthesis *34*
3.2.2. Bisguanidinium disulfide Synthesis *34*
3.2.3. Disulfide Bond Reduction and Purification *35*
3.2.4. Characterization Techniques *35*
3.3. Hydrogel Fabrication 35
3.3.1. Polymer Functionalization *35*
3.3.2. Crosslinking Mechanism *36*
3.4. Functionalization and Characterization of Magnetic Beads 37
3.5. Monitoring protein denaturation 37
3.6. miRNA Extraction and Quantification 38
3.7. Statistical Analysis 38

4. RESULTS AND DISCUSSION 40

4.1. CHARACTERIZATION OF THE SYNTHESIZED GUANIDINE MOLECULES 40
4.2. DENATURING BEHAVIOR OF THE GUANIDINE MOLECULES 40
4.3. HYDROGEL CHARACTERIZATION 42
4.4. EFFECT OF DENATURING HYDROGELS ON PROTEIN'S INTEGRITY 42
4.5. MAGNETIC BEADS CHARACTERIZATION 43
4.6. EFFECT OF DENATURING MBS ON PROTEIN'S INTEGRITY 46
4.7. EFFECT OF MBS ON MIRNA EXTRACTION FROM PLASMA SAMPLES 46

5. CONCLUSION AND PERSPECTIVES 50

6. REFERENCES 53

I. APPENDIX 57

LIST OF FIGURES

FIGURE 2.1 SCHEME OF THE TWO SYNTHESIZED GUANIDINE DERIVATIVES: A) GUANIDINOETHYL AND B) BISGUANIDINIUM. 31
FIGURE 2.2 SCHEME OF THE HYDROGEL MATRIX DENATURING SEQUENCE. 32
FIGURE 2.3 SCHEME OF THE MAGNETIC BEADS DENATURING SEQUENCE. 32
FIGURE 3.1 STRUCTURE OF A) ALGINATE FUNCTIONALIZED WITH MALEIMIDE; B) ALGINATE FUNCTIONALIZED WITH METHACRYLATE AND C) PVA FUNCTIONALIZED WITH METHACRYLATE. 36
FIGURE 3.2 SCHEME OF MBS FUNCTIONALIZATION: A) FIRST STEP OF FUNCTIONALIZATION, ATTACH MALEIMIDE GROUPS TO THE CARBOXYLIC GROUPS, B) CLICK CHEMISTRY TO ATTACH THE BISGUANIDINIUM SULFIDE, C) CLICK CHEMISTRY TO ATTACH THE GUANIDINOETHYL SULFIDE. . 37
FIGURE 4.1 EFFECT OF GUANIDINE DERIVATIVES ON PROTEIN INTEGRITY: A) GUANIDINOETHYL DISULFIDE AND B) BISGUANIDINIUM DISULFIDE. 41
FIGURE 4.2 CIRCULAR DICHROISM OF 1 MM BSA AND DIFFERENT CONCENTRATIONS OF A) GUANIDINOETHYL AND B) BISGUANIDINIUM. 41
FIGURE 4.3 EFFECT OF THE DENATURING MOLECULES ENTRAPPED IN CROSSLINKED ALGINATE DISCS ON PROTEIN INTEGRITY: A) GUANIDINOETHYL DISULFIDE AND B) BISGUANIDINIUM DISULFIDE. 43
FIGURE 4.4 EFFECT OF CLICKED HYDROGEL DISCS ON PROTEIN INTEGRITY: PVA MA (BLUE) AND ALG MA (GREEN). 43
FIGURE 4.5 A) ZETA POTENTIAL ($P<1.0$) AND B) HYDRODYNAMIC DIAMETER OF MBS-COOH, MBS-MALEIMIDE, MBS-GUANIDINOETHYL AND MBS-BISGUANIDINIUM. 45
FIGURE 4.6 FTIR SPECTRA OF BARE MAGNETIC BEADS (BLACK LINE); MBS FUNCTIONALIZED WITH MALEIMIDE (GREY LINE); MBS FURTHER FUNCTIONALIZED WITH GUANIDINOETHYL (GREEN LINE) OR BISGUANIDINIUM (ORANGE LINE). 45
FIGURE 4.7 A) SCHEME ILLUSTRATING THE STEPS TAKEN FOR FLUOROMETRIC ASSAY USING MBS: MIXTURE OF MBS AND A SOLUTION OF BSA-ANS WAS TRANSFERRED TO A MICROPLATE (A MAGNET WAS USED TO SETTLE THE MBS AT THE BOTTOM) AND THE FLUORESCENCE WAS MEASURED USING A PLATE READER; FLUORESCENCE RESPONSE OF THE B) MBS-GUANIDINOETHYL AND C) MBS-BISGUANIDINIUM. 46
FIGURE 4.8 MIRNA RECOVERY OF DIFFERENT EXTRACTION CONDITIONS WAS EVALUATED BY THE CT VALUES ASSAYED IN THE QPCR. 47
FIGURE I.1 A) 1H-NMR SPECTRA OF TETRA-BOC-BISGUANIDINE AND GUANIDINOETHYL DISULFIDE (^{1}H-NMR (D_2O, 400 MHZ): 3.54 (T, J = 6.2 HZ, 4H), 2.91 (T, J = 6.3 HZ, 4H), 1.50 (S, 36H).); B) LC-MS OF THE GUANIDINOETHYL PURIFIED 57
FIGURE I.2 LC-MS SPECTRA OF A) BISGUANIDINIUM DISULFIDE AND B) BISGUANIDINIUM PURIFIED. 58

FIGURE I.3 ABSORBANCE SPECTRUM A) GUANIDINOETHYL AND B) BISGUANIDINIUM. 59
FIGURE I.4 ^{1}H NMR SPECTRA (D_2O, 400 MHZ) OF THE ALGINATE (BLACK LINE); ALGINATE FUNCTIONALIZED WITH MALEIMIDE (GREY LINE, MALEIMIDE CHEMICAL SHIFT AT 6.2 PPM) AND ALGINATE FURTHER FUNCTIONALIZED WITH GUANIDINOETHYL (GREEN LINE). 59
FIGURE I.5 ^{1}H NMR SPECTRA (D_2O, 400 MHZ) OF THE COMMERCIAL ALG MA (BLACK LINE); ALG MA FUNCTIONALIZED WITH BISGUANIDINIUM (ORANGE LINE) OR WITH GUANIDINOETHYL (GREEN LINE). GREY OVALS HIGHLIGHT THE COUPLED MOLECULES.....60
FIGURE I.6 ^{1}H NMR SPECTRA (D_2O, 400 MHZ) OF THE PVA (BLACK LINE); PVA MA (GREY LINE); PVA MA FUNCTIONALIZED WITH BISGUANIDINIUM (ORANGE LINE) OR WITH GUANIDINOETHYL (GREEN LINE). GREY OVALS HIGHLIGHT THE COUPLED MOLECULES.....60

SYMBOLS

pKa	Acidity constant
δ	Chemical shift

ACRONYMS

^{1}H NMR	Proton Nuclear Magnetic Resonance
Alg	Sodium Alginate
ANS	8-Anilinonaphthalene-1-sulfonic acid
BSA	Bovine serum albumin
CD	Circular Dichroism spectroscopy
diH_2O	Deionized Water
DLS	Dynamic Light Scattering
EDC	1-ethyl-3-(3-dimethylaminopropyl)carbodiimide
FTIR	Fourier-transform infrared spectroscopy
LC	Liquid Chromatography
LC-MS	Liquid chromatography–mass spectrometry
LFT	Lateral Flow Test
MA	Methacrylate
MBs	Magnetic beads
miRNA	Micro-Ribonucleic Acid
MS	Mass spectrometry
NHS	N-Hydroxysuccinimide
PBS	Phosphate-buffered saline
POC	Point-of-Care
PVA	Polyvinyl alcohol
RP-HPLC	Reverse-Phase High Pressure Liquid Chromatography
TCEP	Tris(2-carboxyethyl)phosphine
EDL	Electric double layer

1.
MOTIVATION AND OBJECTIVES

Recent global events have enhanced the role that biosensing technologies have in medical diagnostics and disease monitoring, resulting in an increase demand for more convenient sensing platforms. Consequently, the use of point of care (POC) testing has become more and more popular in clinical diagnosis due to its convenience, faster result times, and potential to improve the outcome for the patient. [1]

In order to meet this demand, the selection of biomarkers needs to meet certain criteria. It needs to be accessible, meaning it should only require minimal invasive protocols for extraction; and should be specific to the pathology being investigated. As a result, liquid biopsies are of particular interest. They refer to the molecular analysis of biomarkers present in biological fluids; where sample extraction is minimally or non-invasive. These biomarkers include circulating subcellular structures, as exosomes, and other biomolecules, such as nucleic acids (mainly miRNA and cell-free DNA). [2] In particular, the recently discovered miRNAs have become potential biomarker candidates. miRNAs are a class of short, non-coding RNAs present in several bodily fluids (such as blood, plasma, saliva, etc.), that are also involved in post-transcriptional gene expression. [3] Their dysregulated expression has been implicated the origin and development of a pathology. In addition, different expression profiles of deregulated miRNAs are characteristic of specific diseases, enabling their usage as diagnostic, prognostic but also predictive biomarkers. [3]

Nonetheless, due to their recent discovery, miRNA sensing still faces technical challenges. Their abundance and under which form circulating miRNA exist in different bodily fluids still presents a problem in their detection. [4] In addition, the lack of suitable analytical tools and standardized protocols to detect miRNAs, impairs quantitative comparisons between studies carried out under slightly different conditions. Current commercially available miRNA extraction kits are time consuming, requiring several steps and centrifugations to separate the smaller RNAs; but also rely on toxic reagents, such as phenol and chloroform, for phase separation, limiting the translation to POC devices. [5]

Therefore, the broad objective of this work is to contribute to this challenging issue, presenting different platforms for standardized, on-chip miRNA release. Firstly, guanidine derivatives were engineered to denature proteins and to allow their coupling via Thiol-Michael addition click chemistry. Secondly, two separate systems were hypothesized to incorporate and possibly enhance the denaturing properties of the guanidine derivatives. Various hydrogels and commercially available magnetic beads were functionalized, characterized and tested for protein denaturation. Finally, the magnetic beads system was tested with clinical samples to assess their ability to release miRNAs from carriers in plasma samples. In addition, data analysis and representation were evaluated using Python.

2. INTRODUCTION

2.1. miRNAs as Biomarkers

Micro-ribonucleic acids (miRNAs) are short non-coding, single-stranded sequences of RNA with around 19-25 nucleotides in length. Altered expression of miRNAs has been implicated in many diseases including neurological disorders, immune diseases and a variety of cancers, making them attractive biomarkers. [3]

The biogenesis of miRNA starts in the cell nucleus where is first transcribed as a long RNA molecule, which forms base pairs with itself and folds over to make a hairpin. Next, the hairpin is cleaved, releasing a small double-stranded fragment, referred as pre-miRNA. The pre-miRNA is then transported out of the nucleus through exportins. Now, in the cytoplasm, the pre-miRNA is cleaved into miRNA duplexes with the active strand binding to Argonaute proteins and the inactive strand being degraded. This association allows the miRNA to bind to mRNA and induce gene silencing either through inhibition of mRNA translation or mRNA destabilization. [6] Their presence in these regulatory mechanisms indicates that miRNA expression profiles are often dysregulated as a result of a pathological change. Different expression profiles of deregulated miRNA have been linked to specific diseases, allowing them to be exploited as diagnostic, prognostic and predictive biomarkers. [3]

Furthermore, miRNAs are present in several bodily fluids, such as plasma, serum, saliva and urine. [7] In particular, circulating miRNAs present in blood are highly stable and resistant to RNase activity (enzyme that catalyzes the degradation of RNAs). it has been suggested that they are protected from degradation by being packaged in lipid vesicles (such as microvesicles and exosomes), in complexes with RNA binding protein or both. [8] This availability enables to use noninvasive protocols for sample extraction, making them ideal biomarkers for point-of-care (POC) testing. However, the isolation of these biomarkers presents some challenges. The lack of standardized protocols to isolate miRNAs does not allow to draw quantitative comparisons between studies under different conditions. The nature of the biofluid being tested and also the way the fluid is processed prior to analysis will impose a limitation on detection. [5], [9] As a result, standardizing miRNA isolation in order to reliably detect its concentration from a given biofluid would enable further identification and clinical validation of new miRNA biomarkers, increasing the usefulness and demand for miRNA POC devices.

2.2. miRNA Isolation

MiRNAs are very stable in biological fluids and remain stable after several freeze-thaw cycles, pH, temperature changes and long-term storage. Depending on the bodily fluid analyzed, different miRNAs may be found. However, the transporting mechanism of miRNAs (i.e. circulating in solution, trapped inside exosomes or attached to one or more proteins) for each liquid biopsy remains a challenge. It was suggested by Arroyo *et al.* that the transport mechanism of miRNAs in plasma and serum was mainly Argonaute2 (Ago2) proteins and only a fewer proportion was found in vesicles. [10] This was confirmed by Turchinovich *et al.* when looking into the transport of miRNAs in plasma and cell culture media. [11] However, the findings of Gallo et al. determined that most miRNAs in serum and saliva are actually found within exosomes, contradicting the previous discoveries. [12] This ambiguity in literature regarding the biogenesis of miRNAs impairs its detection. The primary mechanism for detection is PCR based [13], which requires miRNA extraction and purification prior to detection. Depending on the sample in question, different extraction protocols are followed. This not only imposes more steps associated with sample handling which will generate variability, influencing the final concentration and stability of the miRNA extracted, but also inhibit a direct comparison between findings. As a result, the lack of standardized protocols to extract and detect miRNAs, limits its translation as a biomarker.

Currently, one of the most common used methods for miRNAs isolation from bodily fluids is phenol-chloroform phase extraction. This method allows to denature proteins and fraction nucleic acids from proteins, allowing to extract an aqueous phase for further proccessing or purification. In this method, chaotropic salts are often used to assist with protein denaturation. However, multiple steps and handling of toxic reagents are still required, imposing a limitation for POC where samples should be easily and safely handled to allow quick analysis. [14]

Another recurring method for miRNA isolation involves silica-based columns. Once miRNAs have been extracted into an aqueous phase, ethanol is added to increase their affinity to the silica particles. The adsorption of nucleic acids on the silica surface can be regulated with the use of chaotropic agents as well. Following this step, the organic phase is then centrifuged to leave the nucleic acids bound onto the solid phase, allowing elution. [5] However, multiple time-consuming steps are still required, inhibiting its translation into a POC device.

Current miRNA commercial extraction kits are often chemical or column-based, or even both, aiming for faster and more efficient nucleic acid extraction. Nonetheless, the selection of kits is dictated by the sample type, creating significant variability between kits. [14], [15]

2.3. Protein Denaturation - Guanidine Derivatives

Denaturing agents are used to disrupt the three-dimensional structure of native proteins, leading to the loss of their biological functionality and detachment of bound miRNAs. Proteins' stability is known to be strongly dependent on the presence of hydrogen bond networks between solvent molecules. Chaotropic agents may alter the stability of proteins either by binding directly to them or by modifying the properties of the solvent. In this last case, the presence of chaotropic molecules creates a perturbation in the hydrogen bond network between water molecules that also results in weakening of the hydrophobic effect. This effect is what leads to protein denaturation. Additionally, the direct binding of chaotropic molecules to proteins may result in a further weakening of the

hydrophobic interactions between nonpolar amino acids that stabilize the native state of proteins. [16] With the unfolding of proteins, the miRNA is released from the complex and available for detection.

Chaotropic salts, such as guanidine, are widely used in miRNA extraction kits, irrespective of sample type. Guanidine ions bind to polypeptides, which are expected to provide a significant contribution to protein unfolding. The interaction of the amine groups of guanidine with the protein's peptide groups is concentration dependent, requiring typically concentrations in the molar range. [17], [18] Additionally, it has been shown that the effectiveness of several guanidine-derived denaturants increases with alkyl substitution. [17]

2.4. Denaturing Platforms

2.4.1. Hydrogel

Hydrogels have been widely used in biosensing technologies [19], in particular as immobilization matrixes for pre-purification of samples. [20] Due to the hydrophilic functional groups attached to the polymeric backbone, hydrogels possess a high-water content that also enables them to be shaped and structured into various geometries. Additionally, hydrogels can be tuned for a specific application. This is achieved by controlling the chemical composition, crosslinking density, network structure and pore size. [19] Hydrogels can rise from synthetic or natural polymers. Biopolymers possess a plethora of unique properties, including biocompatibility, non-toxicity and biodegradability. Among these biopolymers is alginate, a natural water-soluble polysaccharide. It is characterized as an anionic copolymer comprised of mannuronic acid (M blocks) and guluronic acid (G blocks) units. [21] The physical properties of alginates depend on the relative proportions of the M and G blocks in the biopolymer. Gel formation happens due to the interaction of G blocks in the presence of divalent cations, binding to form tightly interacting nodes (crosslinking). On the other hand, synthetic polymers also present interesting features, such as excellent mechanical properties, controllable degradation rate. Among them, poly(vinyl alcohol) (PVA) is also widely used in hydrogel formulations, because of its solubility in water, biocompatibility and its abundance of modifiable, pendant hydroxy groups. [19] Hence, hydrogels can be tailored in different structures and integrated into systems, depending on their chemical and physical structure.

Recently, a lateral flow test (LFT) with a hydrogel-based sample loading pad was tested for pre-term birth miRNA detection. [22] Here, a cellulose pad was coated with alginate hydrogel loaded with a denaturing agent (SDS), to allow protein unfolding and exosome breakage for further release of nucleic acid biomarkers from both carriers and enable downstream detection. Upon loading of the plasma sample onto the pad, it was observed a significant increase in signal intensity for the SDS loaded hydrogel coated pads, suggesting that miRNAs were released. Based on this sample processing technology, it was here hypothesized that different hydrogel configurations (i.e. polymers and functionalization chemistries) could chemically incorporate the designed denaturants and operate as denaturing platforms, allowing miRNAs to be released for subsequent detection.

2.4.2. Magnetic Beads

Magnetic Beads (MBs) are nano- or microparticles with a metal core that have become a popular choice for protein purification. The beads are superparamagnetic particles, i.e., behave like

magnets when subjected to a magnetic field, yet retain no residual magnetism when the magnetic field is removed. [23] This feature grants them the ability to achieve quick separation, allowing for a more complete supernatant removal without wasting materials or requiring further process steps (e.g. centrifugation). Additionally, MBs surface can be modified depending on their final application, enabling them to be specific to a defined target. This has attracted manufacturers into developing different commercial nucleic acid isolation kits based on MBs. However, these kits still require the use of toxic reagents, several process steps and lab equipment, being time consuming.

Despite this, due to different compositions, sizes and magnetic properties, MBs can be used in a variety of instruments and formats for biosensing, making them an interesting vehicle for sample processing. [24]

2.5. Project Aims

In this study, two separate platforms combining different denaturing agents were engineered with the aim of releasing miRNA from proteins and exosomes. Contributing with tools towards the development of possible platforms for point-of-care devices and to the understanding of difficulties and further steps of action in achieving high quality miRNA extraction.

Firstly, two guanidine derivatives were synthesized and tested for protein unfolding (Figure 2.1). It was hypothesized that an alkyl chain, also present in other denaturants (i.e. sodium dodecyl sulfate), would enhance the denaturing properties of guanidine. However, to keep the working concentrations of denaturant low, a small alkyl chain was designed. Additionally, to study the influence of an extra guanidine group, one of the iterations contained two guanidine groups (Figure 2.1 b)) at the end of the chain, whilst the other only had one (Figure 2.1 b)). Each contained a sulfur group to allow for Thiol-Michael addition click reactions.

a) **b)**

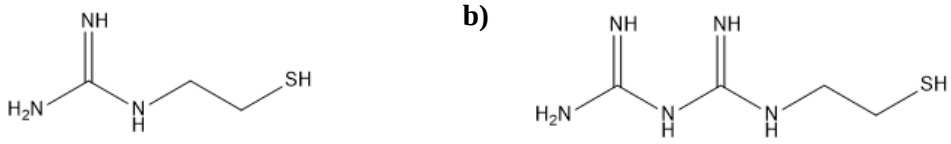

Guanidinoethyl Bisguanidinium

Figure 2.1 Scheme of the two synthesized guanidine derivatives: a) Guanidinoethyl and b) Bisguanidinium.

Alginate and PVA were chosen for hydrogel fabrication. Alginates can be modified on two secondary hydroxyl groups or on the carboxyl group. The difference in reactivity between these two types of functional groups can be used to selectively modify one of the functional groups. Firstly, maleimide (N-(2- aminoethyl) maleimide hydrochloride) was attached to the carboxylic group of alginate. The reaction was promoted by a coupling agents (1-ethyl-3-(3-dimethylaminopropyl) carbodiimide and N-Hydroxysuccinimide) to form amide linkages between the amine group on maleimide and the carboxylate moieties on the alginate polymer backbone (Figure 3.1 a)). A second iteration was also studied, alginate functionalized with methacrylate groups (Figure 3.1 b)), where a commercially available formulation was used. Both maleimides and methacrylate are broadly applicable for coupling with reactive thiol moieties via Thiol-Michael addition click reactions. The maleimide-thiol reaction is still frequently applied in functionalization protocols because of its high selectivity, fast reaction kinetics and mild reaction conditions. [25] The methacrylates, although less reactive than maleimides, have been widely studied for hydrogel functionalization and crosslink. [25],

[26] These modifications allow further attachment of the guanidine derivatives via a thiol bond. PVA was also functionalized with methacrylate groups (Figure 3.1 c)), enabling for further functionalization with the guanidine derivatives and photopolymerization. The hypothesized platforms would enhance the effects observed with the guanidine derivatives, by unfolding proteins entrapped in the three-dimensional network of the hydrogels, thus realizing the miRNAs for downstream detection. (Figure 2.2).

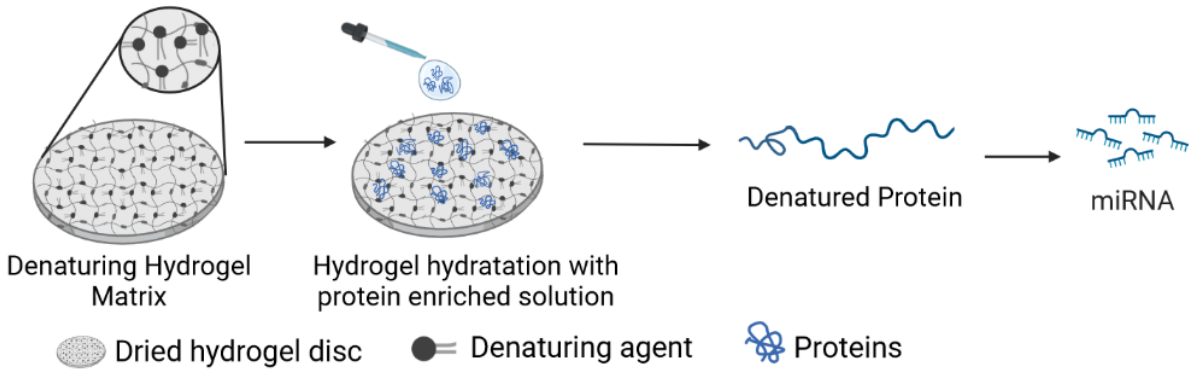

Figure 2.2 Scheme of the hydrogel matrix denaturing sequence.

The second hypothesized platform for miRNA release was based on MBs (Figure 2.3). Here in, commercially available MBs were engineered to unfold proteins and break exosomes, aiming to release miRNA and allow an easy separation method for posterior miRNA detection. The chosen MBs were equipped with carboxylic groups on the surface which were activated using the same carbodiimide chemistry as before, to then attach maleimide groups through covalent bonds. The maleimide terminated beads were then coupled to the produced guanidine derivatives via thiol click chemistry. Therefore, allowing for miRNA extraction for generic applications, rather than targeting a specific miRNA. The engineered magnetic beads were successfully employed in protein unfolding, confirmed by fluorometric assay. Then, the MBs were further tested for miRNA release and quantification, by adapting a current miRNA extraction kit and detection by quantitative polymerase chain reaction (qPCR).

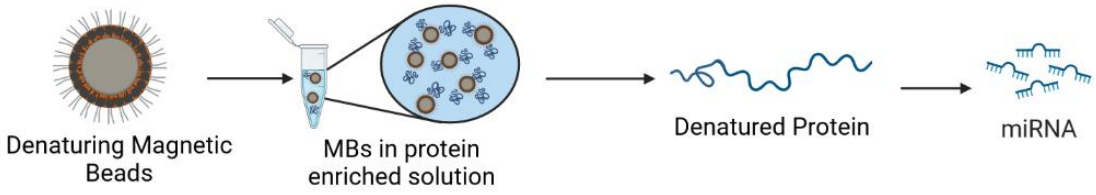

Figure 2.3 Scheme of the magnetic beads denaturing sequence.

3. MATERIALS AND METHODS

3.1. Materials

N-(2- aminoethyl) maleimide hydrochloride and Tris(2-carboxyethyl)phosphine hydrochloride (TCEP) were purchased from Tokyo Chemical Industry UK (Oxford, United Kingdom). tert-Butyl [(tert-Butoxycarbonyl)amino]{[(trifluoromethyl)-sulfonyl]imino}methylcarbamate was purchased from Fluorochem (Derbyshire, United Kingdom). Dynabeads™ MyOne™ Carboxylic Acid (10 mg/ml concentration, 1 µm diameter) were purchased from Thermo Fisher Scientific (United Kingdom). Alginate methacrylate (low viscosity, degree of methacrylation: 10-30 %) and all the other reagents were purchased from Sigma Aldrich (Dorset, United Kingdom). Plasma samples were acquired from TCS Biosciences (Buckingham, United Kingdom) in 2017.

3.2. Synthesis and Characterization of Guanidine Derivatives

3.2.1. Guanidinoethyl disulfide Synthesis

Guanidinoethyl disulfide (Guethyl) was synthesized using the methodology of Nielsen MC *et al*. [27] Briefly, cystamine dihydrochloride (0.040 g, 0.18 mmol) and tert-Butyl [(tert-Butoxycarbonyl)amino]{[(trifluoromethyl)-sulfonyl]imino}methylcarbamate (0.140 g, 0.36 mmol) were suspended in dry dichloromethane (DCM, 3 mL) under a nitrogen atmosphere. Triethylamine (Et_3N, 154 µL, 1.11 mmol) was added and the mixture was stirred for 10 h at room temperature (RT), during which the white solids dissolved.

DCM (15 mL) was added to the mixture and the organic phase was washed with 2 M sodium hydrogen sulfate solution ($NaHSO_4$, 10 mL), saturated sodium bicarbonate solution ($NaHCO_3$, 10 mL), brine (15 mL) and dried magnesium sulfate (MgSO4). The solution was then evaporated to remove the unnecessary solvents.

The tetra-Boc-bisguanidine compound (0.072 g, 0.11 mmol) was dissolved in dry DCM (1.5 mL) under nitrogen and trifluoroacetic (TFA, 300 µL) was added. The mixture was stirred for 1 h at RT and evaporated in the end. To obtain the final product, diethyl ether was added to precipitate the mixture, creating a white powder.

3.2.2. Bisguanidinium disulfide Synthesis

To produce bisguanidinum disulfide (Bisgu), firstly cystamine dichloride (1.126 g, 5 mmol) was ground in a mortar with dicyandiamide (0.84 g, 9.99 mmol) using a mortar and pestle. The

mixture was then heated up to 150 °C in a silicon oil bath under a nitrogen atmosphere for 1 h. The resulting melt was diluted in deionized water (diH_2O) and freeze-dried.

3.2.3. Disulfide Bond Reduction and Purification

The disulfide bond of both guanidine derivatives was broken by dissolving them in diH_2O and adding a 1.5-fold molar excess of TCEP. The solution was left to react for 1 h at RT.

Reverse-Phase High Pressure Liquid Chromatography (RP-HPLC) was used to purify the produced molecules. Once the reduction reaction was complete, the resulting solution was injected into the RP-HPLC. The RP-HPLC system used was from Shimadzu with a C18 column (Gemini 5 µm NX-C18 110 Å, 150x21.2 mm). For the analysis, ultraviolet (UV) detection (Photodiode Array Detector - SPD-M40) was at a wavelength of 254 nm and the flow rate was set to 15 ml/min.

3.2.4. Characterization Techniques

Proton nuclear magnetic resonance (^{1}H-NMR) technique was used to characterize the produced molecules (Bruker Avance III HD standard spectrometer operating at 400 MHz proton; TopSpin software). The spectra were acquired with 16 scans at RT.

Liquid chromatography–mass spectrometry (LC–MS) was used to analyze the main components of the molecules, serving as a more quantitative characterization technique (Q Exactive UHMR Hybrid Quadrupole-Orbitrap Mass Spectrometer (Thermo Fisher Scientific, United Kingdom); C18 silica column (Accucore™ Vanquish™ C18+ UHPLC Columns, 1.5µm)).

3.3. Hydrogel Fabrication

3.3.1. Polymer Functionalization

Alginate maleimide (Figure 3.1 a)) was synthesized as reported by Oki Y *et al* [28]. Commercially available alginate methacrylate (Figure 3.1 b)) was used without any further purification step. PVA methacrylate (Figure 3.1 c)) was synthesized as reported by Bryant SJ *et al.* [29].

To click the denaturants to the hydrogels, 200 g of each polymer were dissolved in 50 ml of diH_2O at 60 °C. Once fully dissolved, 50 g of each denaturant was dissolved in 1 ml of diH_2O and added to each polymer solution. The thiol addition was let to react for 2 h at 60 °C. In the end, the functionalized polymers were dialyzed for 2 days and then freeze dried.

^{1}H-NMR was performed to chemically characterize the functionalized polymers. Polymers were dissolved in D_2O and spectrums were obtained at RT and at 60 °C in the case of the alginates. Degree of functionalization (DF) of Alg MA clicked with denaturants was determined by calculating the ratio of the normalized area of the denaturant peaks to the methacrylate peaks and multiplying by the overall functionalization with methacrylate groups. Similarly, the degree of functionalization of PVA MA was also calculated by the ratio of the normalized area of the methacrylate peaks to the denaturant peaks.

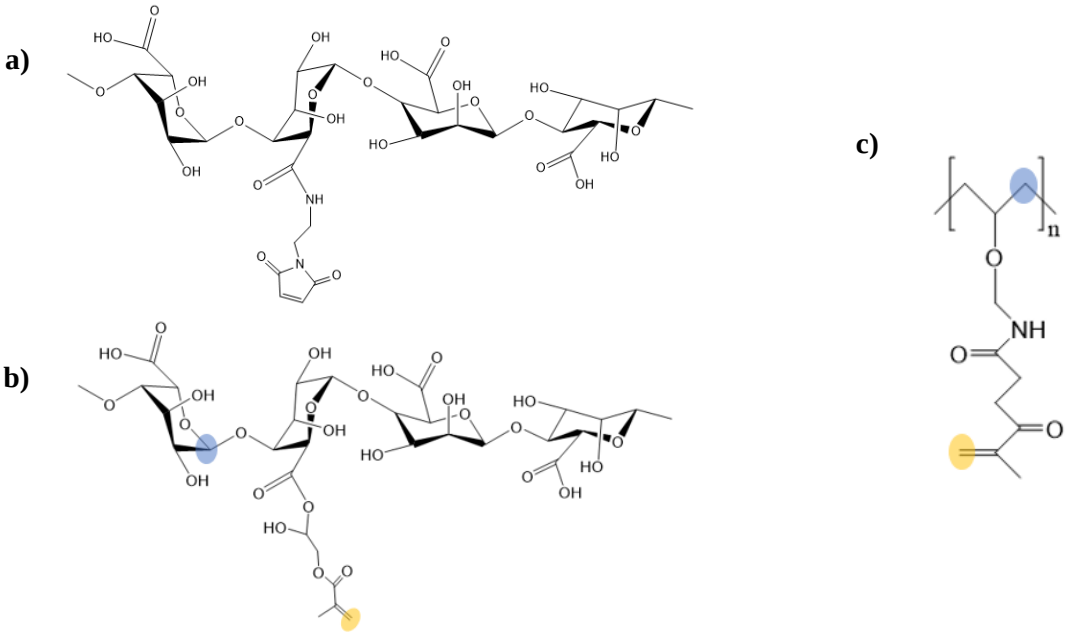

Figure 3.1 Structure of a) alginate functionalized with maleimide; b) alginate functionalized with methacrylate and c) PVA functionalized with methacrylate.

The degree of functionalization of the PVA's structure (DF_{PVA}) with the methacrylate groups (MA) was calculated as expressed by the equation (1):

$$DF_{PVA} = \frac{H_{MA} - H_{PVA}}{H_{PVA}/2} \times 100 \qquad \text{Eq (1)}$$

Where H_{MA} corresponds to the average of the area of the two peaks associated with the protons of the MA groups highlighted in yellow on Figure 3.1 b) and c); and H_{PVA} is the area of the peak associated to the two protons present in PVA's backbone (highlighted in blue on Figure 3.1 c)). The degree of functionalization of the commercially available Alg MA was around 30 %.

The degree of functionalization of the MA groups (DF_{MA}) of the hydrogels with the synthesized molecules was calculated as expressed by the equation (2):

$$DF_{MA} = \frac{H_{MA} - H_{MA-X}}{H_{MA}} \times 100 \qquad \text{Eq (2)}$$

Where H_{MA} is the same as described above and $H_{MA\text{-}X}$ corresponds to the area of the peak associated with the MA groups functionalized with the respective molecules. It was assumed that with the functionalization of the MA groups, less MA groups are available in the whole polymer structure and, therefore, the peak's intensity will decrease. To enable a comparison between the spectrums, the peak associated with two protons present in each of the polymer's backbone was normalized to 2 (highlighted in blue in Figure 3.1 b) and c)).

3.3.2. Crosslinking Mechanism

For the crosslinking mechanism of alginate (3 %wt/v), a slow gelling mechanism was selected and performed as reported by A. E *et al.* [30].

The UV-photopolymerization was used for photocrosslinking AlgMA. Briefly, Alg MA (3 %wt/v) was dissolved in diH_2O at 60 °C and Irgacure 2959 (0.1 %wt/v) was added. The solution was then irradiated with UV light in a BLX-315 UV crosslinker (315 nm, 3 min, 1 J energy). PVA MA (10 %wt/v) crosslinking followed the Alg MA's protocol.

After crosslinking, hydrogels discs (10 mm diameter, 10 mm height) were cut using a piercing puncture biopsy and freeze dried.

3.4. Functionalization and Characterization of Magnetic Beads

Functionalization of the MBs with maleimide was performed using EDC/NHS reaction (Figure 3.2 a)), the protocol followed was adapted from Meng X *et al*. [31]. First, 0.5 ml of Dynabeads™ MyOne™ Carboxylic Acid were washed three times with 1x PBS containing 0.01 % Tween surfactant. Then the MBs were resuspended in 1 ml 1x PBS containing 43 mg of EDC and 48 mg of NHS. Following 15 min activation, under constant shaking (1000 rpm), 24 mg of N-(2- aminoethyl) maleimide hydrochloride (maleimide) was added, saturating the carboxylic acid groups available on the MBs surface. The reaction was left under constant shacking (1000 rpm) for 3 h at RT. Once the reaction was complete, the MBs were washed three times with 1xPBS containing 0.01 % Tween surfactant. Then, they were resuspended in the same buffer and stored at 4 °C.

To click the denaturants to the MBs, 30 g of each denaturant (Guethyl, Figure 3.2 b); and Bisgu, Figure 3.2 c)) was dissolved in 1 ml of diH_2O. The MBs were resuspended in the denaturant solution and the thiol addition was let to react for 2 h at RT. In the end, the functionalized MBs were washed three times with 1x PBS, then resuspended in the same buffer and stored at 4 °C.

Dynamic Light Scattering (DLS) and Zeta Potential measurements were conducted using the Malvern Zetasizer Pro Blue. Fourier-transform infrared spectroscopy (FTIR) was performed on an Agilent Cary 630 FTIR spectrometer.

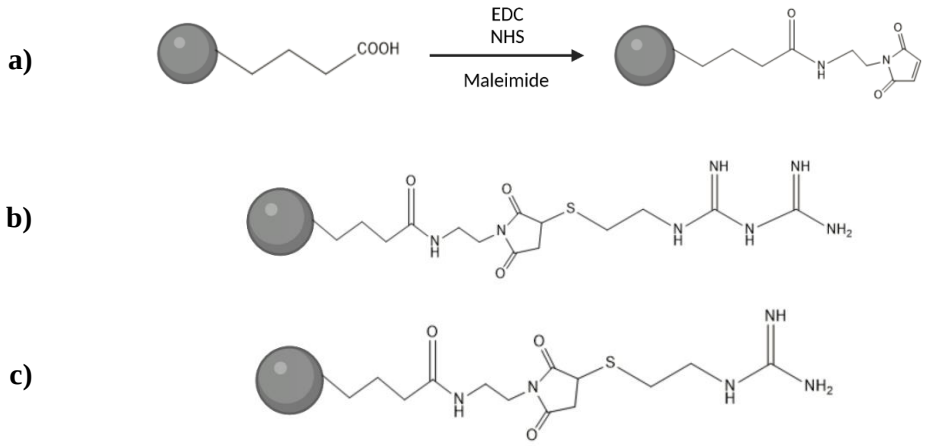

Figure 3.2 Scheme of MBs functionalization: a) first step of functionalization, attach maleimide groups to the carboxylic groups, b) click chemistry to attach the bisguanidinium sulfide, c) click chemistry to attach the guanidinoethyl sulfide.

3.5. Monitoring protein denaturation

A solution of 40 µM bovine serum albumin (BSA) and 4 µM 8-anilino-1-naphthalenesulfonic (ANS) in 1X phosphate-buffered saline (PBS) was prepared, following a protocol described elsewhere to investigate protein denaturation, as fluorescence caused by the binding of ANS to BSA has been reported to drop when the protein structure unfolds. [32] The fluorescence change was detected using a CLARIOstar Plus plate reader (BMG Labtech), with an excitation wavelength of 380 nm and emission of 470 nm.

Different concentrations of denaturants were dissolved in PBS and tested on a 96 microwell black plate. To test the behavior of the denaturants in hydrogel solution, different concentrations of denaturants were mixed in an alginate solution with a final concentration of 1 %wt/v.

Hydrogel discs were tested in a 96 clear bottom microwell black plate with light emission coming from the bottom. The discs were hydrated with 15 μl the ANS-BSA solution.

The MBs platform was tested on a 384 microwell black plate using a volume of 30 μl per well. Several concentrations of MBs were mixed with ANS and BSA (using the same concentrations as above) and the fluorescence was measured after the MBs settled at the bottom of the well. MBs-COOH in PBS solution (1 mg/ml) were also used as a control group.

3.6. miRNA Extraction and Quantification

The miRNA extraction from plasma was performed using the miRNeasy Serum/Plasma Advanced Kit (Qiagen, Manchester, United Kingdom). For the positive control, the protocol was followed as described by the company, whilst for the negative control, the lysis step was not performed (i.e. the buffers RPL and RPP were not added). For the MBs, the lysis step was replaced by the MBs (2 mg/200 μl). Briefly, the beads were added to the 200 μl plasma sample and shaken for 6 min. Then the MBs were removed using a magnet and 1 volume of isopropanol (IPA) was added (as described in the protocol). Following the addition of IPA, both samples (including the negative control) were spined to separate the precipitate from the supernatant. Then, the protocol was followed as described by Qiagen.

Concentration of extracted miRNA was assessed through quantitative Polymerase Chain Reaction (qPCR) as described by Teenan O. *et al.* [33]. The qPCR was performed on the QuantStudio 5 (Thermo Fisher Scientific) and the miRNA analyzed in this study was the hsa-miR-21.

3.7. Statistical Analysis

The averages within each group were tested for normality and compared using two tailed student t-tests where $p<0.05$ was considered statistically significant. Statistical analysis was conducted on Python 3.9 (library: statannot 0.2.3).

4.
RESULTS AND DISCUSSION

4.1. Characterization of the Synthesized Guanidine Molecules

The guanidinoethyl disulfide was synthesized as described in the materials and methods and purified by Reverse-Phase High Pressure Liquid Chromatography (RP-HPLC). ^{1}H-NMR was then used to confirm the successful synthesis. Spectra were recorded before (Figure I.1 a), in appendix) and after the removal of the protecting groups and were consistent with those previously reported by Nielsen MC *et al* [27]. Liquid chromatography–mass spectrometry (LC-MS) was finally used to characterize the purified molecule after reduction of the disulfide bond with TCEP. LC-MS combines the physical separation capabilities of liquid chromatography (LC) with the mass analysis capabilities of mass spectrometry (MS), increasing MS's potential to identify and quantify the analyte of interest. The spectra showed a high intensity peak at a mass of 120.06 g (Figure I.1 b), in appendix) which corresponds to the guanidinoethyl (molecule A), confirming a successful synthesis and purification.

Similarly, the bisguanidinium disulfide was synthesized as described in the materials and methods and purified by RP-HPLC. LC-MS was then used to confirm the successful synthesis. Spectra were recorded before and after the purification step of bisguanidinium disulfide. The initial spectra showed a high intensity peak at a mass of 321.14 g, corresponding to the bisguanidinium disulfide, but also some impurities of partially reacted reagents and other contaminants (Figure I.2 a), in appendix). Once purified, the LC-MS spectra clearly showed a well-defined peak at a mass of 162.08 g (Figure I.2 b), in appendix), confirming a successful synthesis and purification of the bisguanidinium (molecule B).

4.2. Denaturing Behavior of the Guanidine Molecules

The denaturing properties of the molecules A and B were first tested on BSA using either a fluorometric assay or Circular Dichroism (CD) spectroscopy. The unfolding of BSA in buffer solution was firstly observed in a fluorescence-based assay using ANS as a fluorophore, since it has been widely used to characterize protein binding sites in BSA. [34] ANS has high fluorescence activity when bound to the hydrophobic sites of proteins. Upon protein's unfolding, original hydrophobic pockets where ANS molecules were bound start getting exposed to water, decreasing the fluorescence. Both molecules induced BSA's unfolding, as observed by the decrease of fluorescence in Figure 4.1. Higher concentrations of B were required to achieve significant decays in fluorescence, hence BSA unfolding. However, both denaturants performed better at mM concentrations when comparing to guanidinium hydrochloride, that requires M concentrations to achieve similar fluorescence readouts. [32]

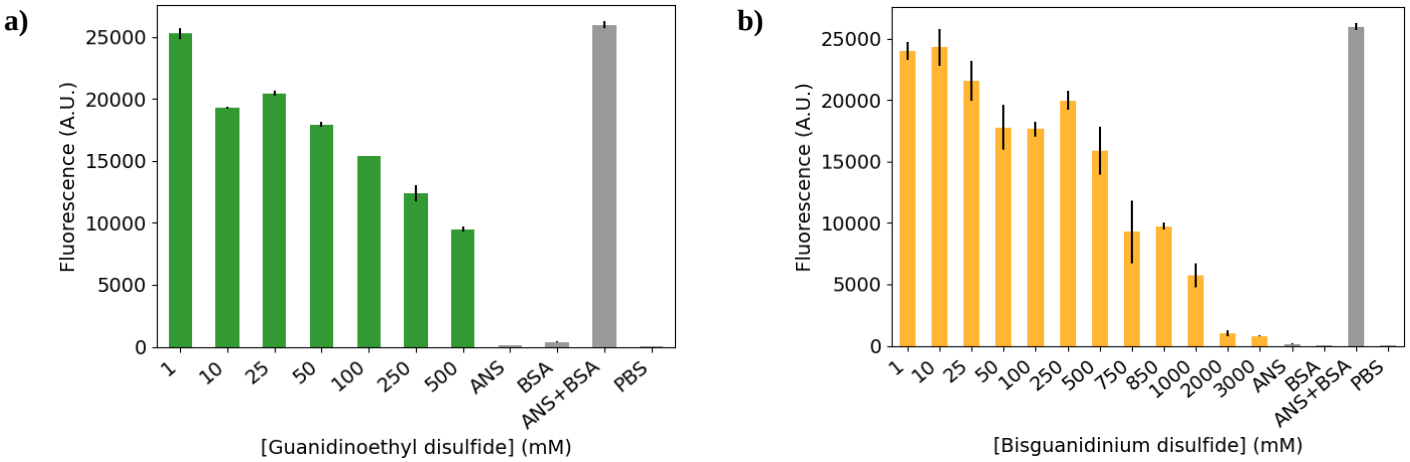

Figure 4.1 Effect of guanidine derivatives on protein integrity: a) guanidinoethyl disulfide and b) bisguanidinium disulfide.

This results were further confirmed by Circular Dichroism (CD) spectroscopy. CD is commonly used to monitor the structure, conformation and stability of proteins in solutions. [35] The secondary structure of proteins presents a peptide bond that is asymmetric and therefore this phenomenon can be seen in CD, since CD measures the differential absorption of left- and right-circularly polarized light. Only working concentrations of both denaturants, based on the fluorometric assay, were studied by CD.

The CD spectrum of native BSA presents as a well-shaped curve with two double-minimum values near 210 and 220 nm (Figure 4.2), which are representative of the α-helix structure of the protein. With the addition of denaturant, the well-shaped curve becomes less pronounced. This behavior is representative of the loss in helical content of BSA which happens upon protein unfolding.

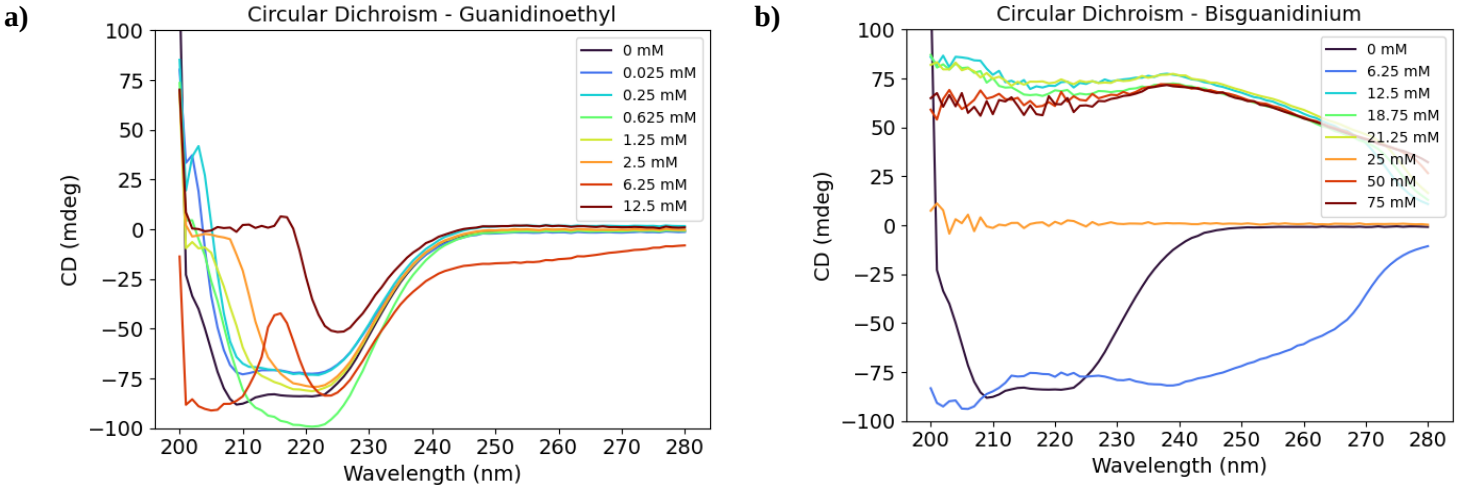

Figure 4.2 Circular Dichroism of 1 μM BSA and different concentrations of a) guanidinoethyl and b) bisguanidinium.

However, due to the carbonyl moieties present in guanidinium, this molecule has high absorbance in the ultraviolet (UV) region at its working concentration. This presents a challenge when monitoring transitions through secondary structure loss by CD, where α-helical structure is detected at 220 nm. In the case of the guanidinoethyl, the inversion of the curve was only observed at higher concentrations of denaturant. Conversely, in the case of bisguanidinium the spectrum conclusions were difficult to extract. This could be due to the second guanidinium group present in the molecule,

which increased the UV absorption (Figure I.3 in appendix) and therefore masks the protein CD spectrum.

4.3. Hydrogel Characterization

Polymers functionalization was characterized by ^{1}H-NMR. The spectra obtained for alginate maleimide showed a small peak (almost indistinguishable from the background noise), suggesting the functionalization was not successful. As a result, alginate maleimide was not used in further experiments.

On the other hand, the alginate methacrylate (Alg MA) functionalization with each molecule (Figure I.5, in appendix) was achieved. The peaks associated with the methylene protons (δ = 6.8 and 6.4 ppm) of the methacrylate groups decrease in intensity, as expected. For the Alg MA functionalized with the molecule A, the functionalization of the methacrylate groups, calculated using equation (2) in the materials and methods section, was 76.5 %. Additionally, two high intensity peaks appeared at 4.1 and 3.7 ppm, which belong to the protons present in the guanidine group of the molecule. For the molecule B, the obtained degree of functionalization (DF_{MA}) of the MA groups in AlgMA was 64.5 %. New peaks also emerged (δ = 4.2 ppm, 3.1 ppm and 2.8 ppm), suggesting the presence of the molecule in the polymer's structure.

The PVA methacrylate modification was also confirmed by ^{1}H-NMR (Figure I.6). The peaks associated with the methylene proton (δ = 6.1 and 5.7 ppm) and the methyl proton (δ = 2.7 ppm) of the MA groups appear in the PVA MA's spectrum, the DF_{PVA} calculated was 1.65 %. Upon the addition of molecule A, the functionalization of the MA groups, calculated using equation (2) in the materials and methods section, was 6.0 %. Additionally, new peaks (δ = 2.6 and 2.5 ppm) associated with the guanidine group of molecule A appeared. For PVA MA functionalized with molecule B, the DF_{MA} of the MA groups was 0.67 % and a low intensity peak was observed at 2.3 ppm.

4.4. Effect of Denaturing Hydrogels on Protein's Integrity

The denaturing properties of selected concentrations of both molecules were then tested in crosslinked alginate discs. Similar fluorometric assay was used to access protein's integrity when entrapped in the hydrogel's matrix as well as the molecules properties in different environments. The results followed a similar trend as before (Figure 4.3). Demonstrating that both molecules, A and B, retain their denaturing properties when embedded with a 1 %wt/v alginate hydrogel. Although a decrease in fluorescence was obtained when comparing the same concentrations to the fluorometric assay in buffer solution. These promising results may be related to the hydrogel's matrix. At this concentration, alginate's porosity should be relatively high and with uniform pore size [30], due to the lower concentrations of crosslinkers that slow gelation. Slowing down gelation allows for the crosslinking to happen throughout the whole volume of the gel, generating a more uniform mesh structure that would enable a more homogeneous hydration. [30] As a result, by entrapping the denaturant and proteins inside, the denaturation may happen in a more concentrated and localized manner. This behavior could then be translated in a better yield when comparing to the buffer solution experiment.

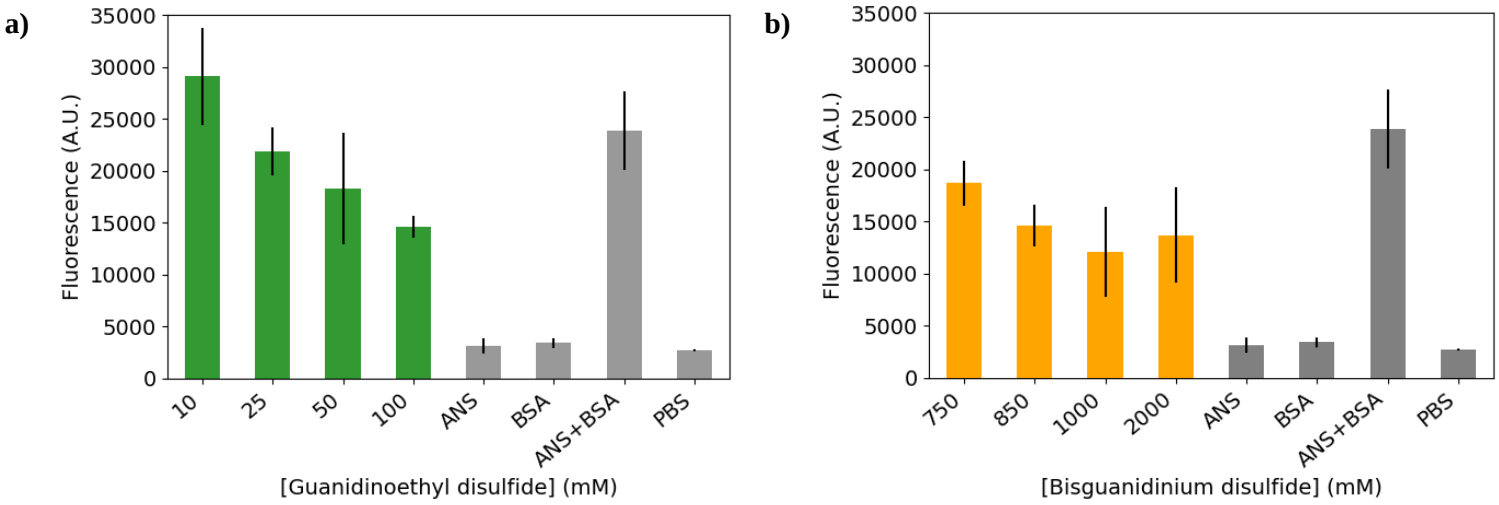

Figure 4.3 Effect of the denaturing molecules entrapped in crosslinked alginate discs on protein integrity: a) guanidinoethyl disulfide and b) bisguanidinium disulfide.

The same fluorometric assay was then performed on the different polymer-based hydrogels with the molecules clicked to their structure (Figure 4.4). Similarly, a decrease in fluorescence was observed in the denaturing discs, meaning that the denaturants were successfully incorporated in the polymer's structure and that their activity was preserved after the processing steps that followed the click reaction (i.e. dialysis, freeze drying and crosslinking by UV exposure). The PVA MA (Figure 4.4 blue bars) performed better in comparison to the Alg MA (Figure 4.4 green bars), resultant of the higher polymer concentration used for the discs' fabrication. This may have created a localized denaturing activity inside the discs, enhancing protein's unfolding and decreasing the fluorescence emission.

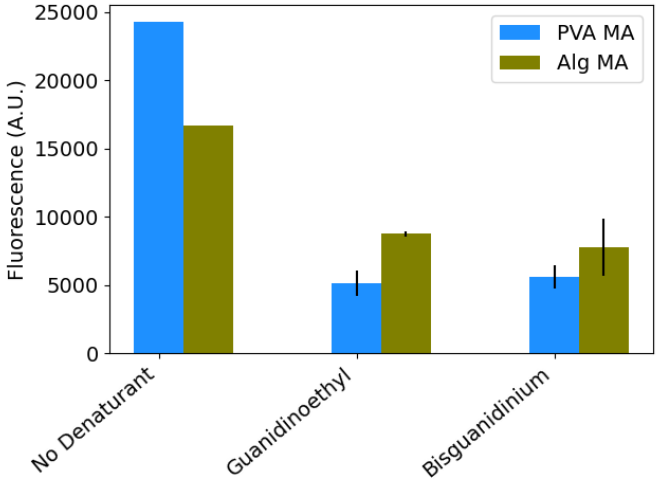

Figure 4.4 Effect of clicked hydrogel discs on protein integrity: PVA MA (blue) and Alg MA (green).

4.5. Magnetic Beads Characterization

Once the denaturing properties of the molecules were tested and their ability to react via thiol-click chemistry was confirmed, they were incorporated onto the magnetic beads (MBs) surface. The commercially available carboxylate magnetic beads (Dynabeads® MyOne™ Carboxylic Acid) were

selected due to their uniform shape, small size (1 μm diameter) and monodispersed properties, which ensure highly reproducible reaction kinetics and efficient binding of functional groups. Their size is of particular interest since it provides a high surface area while keeping the magnetic properties, all suitable for protein interactions. [36] The COOH groups present on the beads surface confer hydrophilic properties that allow for gentle coupling of ligands and stability in aqueous environment. To introduce maleimide functional groups, carbodiimide activation was used to introduce the amide groups needed for the coupling. [37]

The MBs were functionalized as described in the materials and methods section. To characterize the surface modification, zeta potential (ZP, Figure 4.5 a)) and hydrodynamic diameter (Figure 4.5 b)) of the different MBs were measured by light dispersion techniques. Dynamic Light Scattering (DLS) measures Brownian motion and relates it to the size of the particles. The hydrodynamic diameter is then calculated through the Stokes-Einstein equation, which depends also on the viscosity and temperature of the solvent. [38] On the other hand, the ZP is the potential difference between the electric double layer (EDL) of the particle and the layer of the dispersion medium. Consequently, ZP only provides an indication towards the nature of the surface charge (positive/negative), assuming that the predominant ions in the potential interval are similar to the particle's surface. [38]

Starting with the bare MBs (MBs COOH), the carboxylic acid groups present on the surface are negatively charged (Figure 4.5 a) black bar). With the addition of the maleimide groups, the bead's surface should become slightly less negative, as observed by the increase in the zeta potential value (Figure 4.5 a) grey bar). Finally, the coupling of the guanidine derivatives should increase the ZP even more, since the amine groups present on the guanidine structure are basic and therefore, more positively charged (Figure 4.5 a) green bar). However, the trend was not observed in the case of molecule B (Figure 4.5 a) orange bar), which could be due to several reasons. Guanidine has different tautomers, meaning that the C=N double bound can resonate through each of the secondary amines present. Tautomerization can change the bond order of a given bond, and hence the bond length dramatically. For bisguanidines, additional tautomers are possible due to the extra guanidine group. This can lead to difficulties in predicting the pKa of guanidines. [39] The pKa is the pH at which half the acidic groups are protonated, influencing ZP measurements. [38] Additionally, it has been shown that guanidine disturbs the water molecules close to it, when dissolved in this media. Electrostatic interactions take place due to the hydrogen bond, which could lead to variability in the zeta potential results. [40] As a result, the second guanidine group in the MBs-Bisguanidinium will only enhance this behavior, limiting the conclusions that could be drawn from the ZP measurements.

Additionally, the hydrodynamic diameter of the MBs decreases at each functionalization (Figure 4.5 b)). Since commercially available MBs were used, this trend is not representative of the real diameter of the particles. The hydrodynamic diameter depends on variables like temperature, viscosity of the medium and velocity of the Brownian motion (translational diffusion coefficient, D). The latter, not only depends on the size of the particle core, but also on the surface structure. Changing the particle's surface, may affect the diffusion speed which will further change the apparent size of the particle. With each successive functionalization, the particle's surface will be a mix of functional groups, since the yield is not 100 %. As a result, the difference in surface charge may speed the particle's Brownian motion and therefore reduce its hydrodynamic diameter.

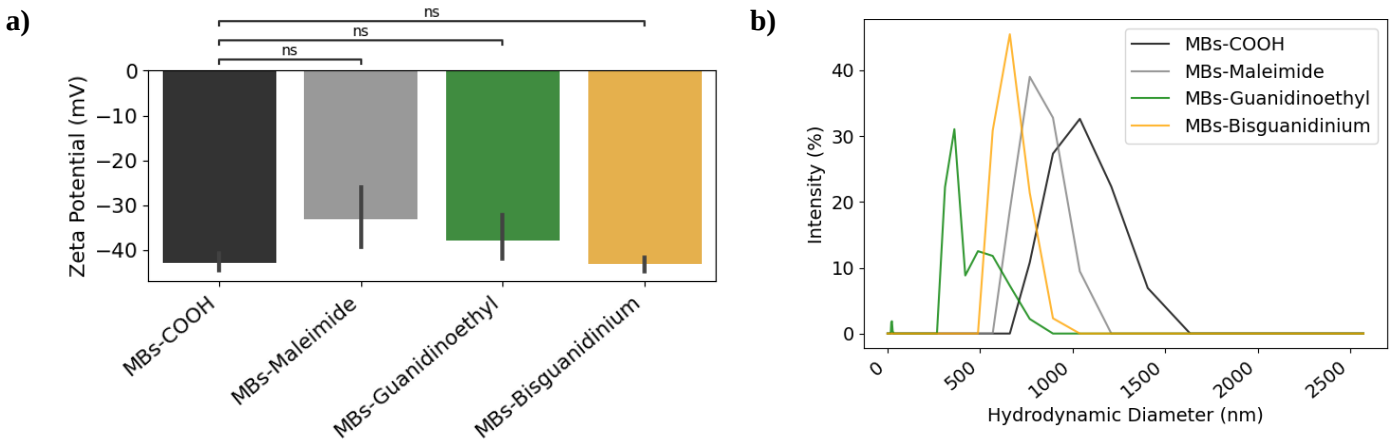

Figure 4.5 a) Zeta Potential (p<1.0) and b) Hydrodynamic Diameter of MBs-COOH, MBs-Maleimide, MBs-Guanidinoethyl and MBs-Bisguanidinium.

Fourier-transform infrared spectroscopy (FTIR) of the magnetic beads was performed on each stage of the functionalization. The FTIR spectrum of each of the MBs (Figure 4.6) is dominated by the absorption peak associated with Fe-O stretching (at 560 cm^{-1}) from the core of the MBs, O-H bending (at 1345 cm^{-1} and 750 cm^{-1}) and the C=O stretching (at 1519 cm^{-1}) belonging to the carboxylic acid end group. The addition of the maleimide group (Figure 4.6 grey line) made the O-H bend (at 750 cm^{-1}) disappear and a new peak associated to C=C stretch of the maleimide molecule appears, at 1706 cm^{-1}. Demonstrating that the -OH group in the carboxylic acid group was functionalized. Upon addition of molecule A (Figure 4.6 green line), the previously observed C=C stretch disappears and an increase in the well-shaped curve occurs on the left side of the spectrum (around 3300 cm^{-1}) as well as a very slight increase on the right side of the spectrum (around 1635 cm^{-1}), indicating that amine groups were introduced in the structure. This is more evident in the MBs-Bisguanidinium case (Figure 4.6 orange line), since it possesses a second guanidine group, corresponding to the introduction of two extra amine groups.

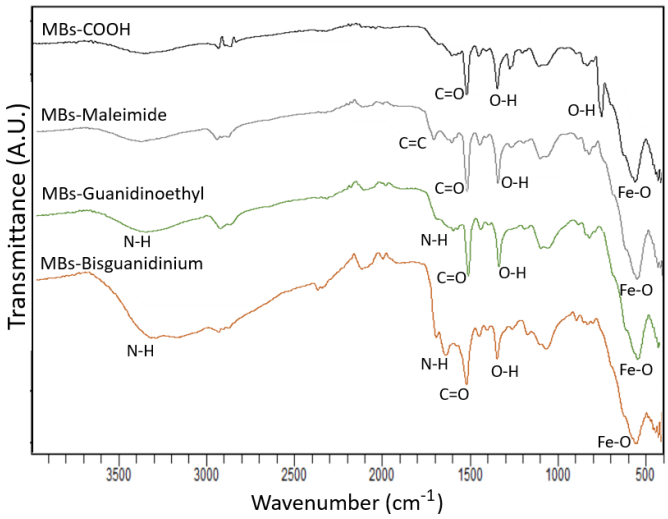

Figure 4.6 FTIR spectra of bare magnetic beads (black line); MBs functionalized with maleimide (grey line); MBs further functionalized with guanidinoethyl (green line) or bisguanidinium (orange line).

4.6. Effect of Denaturing MBs on Protein's Integrity

Denaturing properties of the functionalized magnetic beads were investigated using a fluorometric assay. Initially, the assay was conducted after removing the MBs through magnetic separation. Although, the fluorescence intensity measured was not compliant with the previous trends, i.e., the fluorescence did not decrease with the increase of denaturant added. Upon removal of the MBs, the stimulus for denaturation is removed. Therefore, by removing the MBs, the denaturing agents (clicked molecules) were removed as well. As a result, BSA refolds and the high intensity fluorescence measured corresponds to the ANS binding. This behavior has been previously demonstrated [41], [42], by removing the guanidine denaturant, BSA returns to its folded state. Consequently, different conditions were applied to the experiment. Instead of magnetically separating the solution from the MBs, the whole system was pipetted into each well. Then a magnet was used to help settle the MBs to the bottom (Figure 4.7 a)). This adjustment resulted in the desired trend (Figure 4.7 a) and b)), showing that the engineered system unfolds BSA and proving that the MBs were indeed functionalized with the guanidine derivatives. As expected, the MBs-Bisguanidinium require higher concentrations to achieve similar BSA unfolding in comparison to the MBs-Guanidinoethyl.

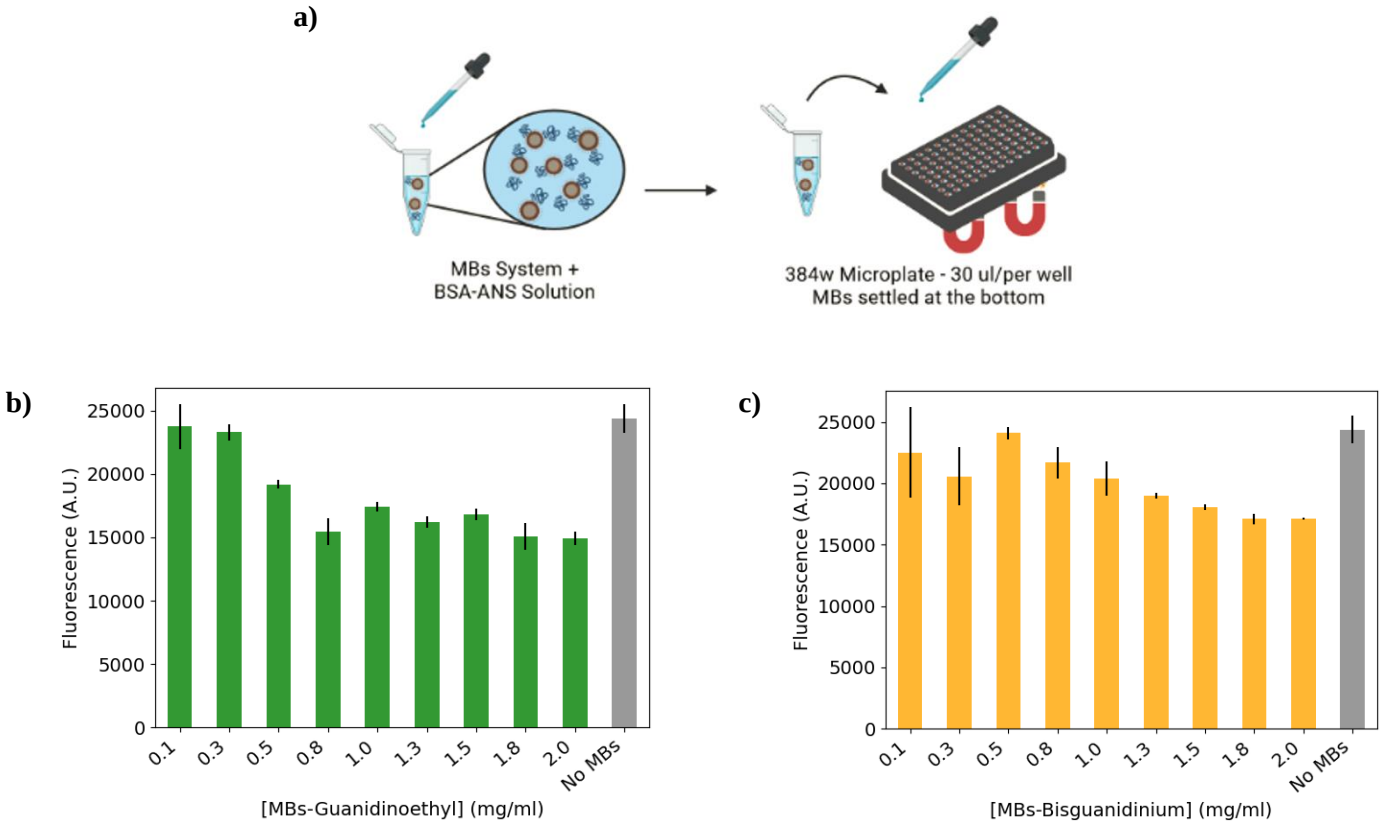

Figure 4.7 a) Scheme illustrating the steps taken for fluorometric assay using MBs: mixture of MBs and a solution of BSA-ANS was transferred to a microplate (a magnet was used to settle the MBs at the bottom) and the fluorescence was measured using a plate reader; fluorescence response of the b) MBs-Guanidinoethyl and c) MBs-Bisguanidinium.

4.7. Effect of MBs on miRNA Extraction from Plasma Samples

The performance of the denaturing MBs in miRNA extraction from plasma samples was accessed by comparing the cycle threshold (CT) values obtained in qPCR (Figure 4.8). In the qPCR, a fluorescent dye is added, enabling to detect fluorescence in real time as the thermal cycler runs, giving

readings throughout the amplification process of the PCR. The CT is defined as the number of cycles required for the fluorescent signal to cross the threshold (i.e. exceeds background level). The CT levels are inversely proportional to the amount of target miRNA in the sample, meaning the lower the CT value, the greater the amount of target miRNA in the sample.

The target miRNA investigated was miR-21. This miRNA is relatively abundant in several bodily fluids, including plasma, and its expression is not specific to a disease, therefore it should be present in a given sample. [43] As a result, the CT for miR-21 present in the positive control (Figure 4.8 black bar), where no alterations to the extraction protocol were made, presented the lowest value ($CT_{positive}$=26). In contrast, the negative control (Figure 4.8 grey bar), where denaturation was skipped, required ten more cycles ($CT_{negative}$=36) to achieve some significant miR-21 quantification. By removing the denaturation step in the beginning of the extraction, miRNA carriers (such as proteins and exosomes) were not denatured and the RNA degradation enzymes (RNase) were not inhibited. As a result, only miRNA already free in solution and that was not degraded by RNases was available for extraction. The replacement of the provided lysis buffers with the MBs, resulted in CT values higher than the obtained for the positive control, as expected. The MBs functionalized with molecule A (Figure 4.8 green bar, CT_A=34) presented a better performance than the MBs functionalized with molecule B (Figure 4.8 orange bar, CT_B=35). In PCR, the number of target miRNA molecule doubles after each cycle [44], which means that miRNA recovery from the MBs was fourfold and twofold higher than the negative control, for the MBs-Guanidinoethyl and MBs-Bisguanidinium respectively.

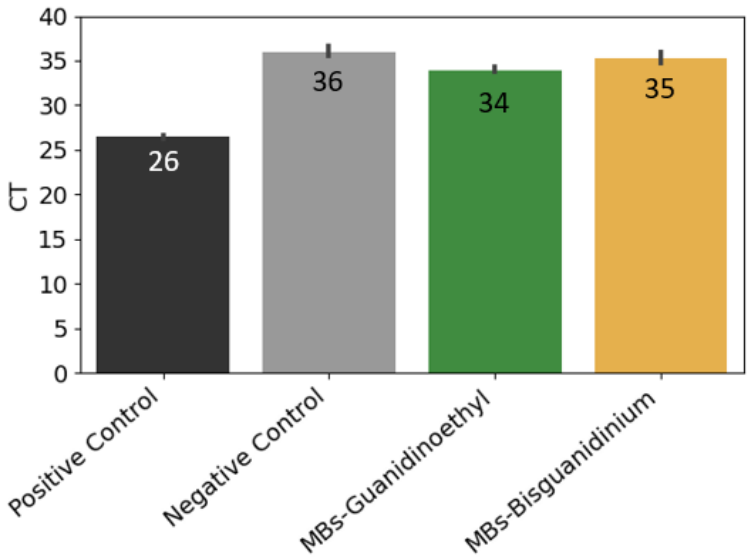

Figure 4.8 miRNA recovery of different extraction conditions was evaluated by the CT values assayed in the qPCR.

In comparison to the positive control, the difference in CT values is much higher. Which is consistent with the fact that the precipitation of plasma components, such as proteins, lipids and carbohydrates, was not performed in the same step sequence as the positive control. Therefore, possible debris could have still been present in the sample. Also, residues of MBs could also have been introduced during the separation step, impairing high-purity samples. Sample purity becomes even more important when dealing with low amounts of miRNA. [13] Considering, that the abundance of miRNA in plasma is lower in comparison to cells and tissues [13] and that plasma frozen for long periods

of time has a decrease in miRNA concentration [45], the resulting miRNA present in the initial sample could have been lower. As a result, the low amount of miRNA coupled with possible low purity samples extracted using the MBs may have constrained the qPCR measurements.

5. CONCLUSION AND PERSPECTIVES

The detection and quantification of miRNAs from bodily fluids holds enormous potential as diagnostic biomarkers for a variety of pathologies, including the early diagnosis of life-threatening diseases, such as cancers. However, miRNA biogenesis is still not fully understood, the lack of standardized protocols and technologies for sample processing limits the translation of miRNA as biomarkers into POC devices. Therefore, standardized methods for miRNA extraction that enable on-chip release, were investigated.

In this study, guanidine derivatives were synthesized with the purpose of allowing protein denaturation. After complete characterization and purification of both molecules (guanidinoethyl and bisguanidinium), fluorometric assay and CD were performed to test their denaturing properties. Both molecules successfully unfolded proteins at mM concentrations, presenting a better performance in comparison to other widely used denaturing agents. [32], [35]

After the incorporation of these molecules on the functionalized hydrogels (PVA MA and Alg MA), fluorometric assay was also used as an analytical tool to study protein unfolding. The denaturing hydrogel matrixes were hydrated with a protein enriched solution and a significant decrease in fluorescence was observed, suggesting the protein structure unfolded. It was also observed that the molecules properties were enhanced by the hydrogel matrix, indicating that their tight mesh creates localized denaturing conditions that increase their yield. Allowing for lower amounts of these guanidine molecules to be used, decreasing the quantity of toxic reagents needed. A key aspect in current miRNA extraction protocols, is that they rely on toxic reagents as phenol-chloroform, for phase extraction; and guanidine thiocyanate solutions, to enable cell lysis. Therefore, by chemically attaching the denaturing molecules into the hydrogel structure, not only lower concentrations of denaturants are required, but also their hazardous activity is not directly exposed.

To allow this mechanism to be further used for clinical sample testing, optimization of the hydrogels' functionalization and ideal polymer concentration should be studied in order to better enhance denaturation, since clinical samples will introduce a more complex environment. Additionally, it would be of great interest to carry out degradation studies. Since to enable its use into POC devices, this mechanism should be stable under a set of conditions.

Next, due to the successful results obtained for the denaturing molecules and hydrogels, it was also considered the use of magnetic beads (MBs) for denaturing and extraction purposes. The commercially available Dynabeads™ MyOne™ were functionalized to incorporate the synthesized molecules on their surface. Functionalization of the MBs with the denaturants was confirmed by several characterization techniques. The MBs were then tested for protein denaturation, the

fluorometric assay caried out showed that the MBs unfolded the proteins. Although, by magnetically separating the MBs from the solution, the proteins that once unfolded began to refold. Suggesting that the refolding mechanism is fast upon removal of the denaturing stimulus.

The MBs were then incorporated in a commercial miRNA extraction kit, by substituting the lysis buffer provided with the MBs. The extraction of miR-21 from plasma using the MBs and required less centrifugations, enabled easier phase separation extraction and carrier breakage without requiring toxic reagents. However, the CT values obtained by qPCR for the MBs (34 and 35 for MBs with molecule A and B, respectively) were closer to the negative control group (no lysis buffer used, $CT_{negative}$=36) than the positive control (manufacturer's protocol was followed, $CT_{positive}$=26). Nonetheless, CT values differed from the negative control group, indicating that miRNA concentration obtain with the MBs was slightly higher. To further improve and automate this miRNA extraction mechanism, improvements in the extraction protocol should be made to better enhance the MBs properties. Aiming for miRNA realize regardless of sample type and limited processing steps.

In conclusion, the denaturing molecules and the miRNA extraction systems engineered here should encourage future trials to explore not only the extraction accuracy of miRNA from clinical samples but also the translation into POC devices.

6. REFERENCES

[1] D. Al Sulaiman, I. Steer, S. Pavagada, and S. Ladame, *Device engineering*. Elsevier Ltd., 2019.

[2] M. Macías *et al.*, 'Liquid Biopsy: From Basic Research to Clinical Practice', *Adv. Clin. Chem.*, vol. 83, pp. 73–119, Jan. 2018, doi: 10.1016/BS.ACC.2017.10.003.

[3] J. Wang, J. Chen, and S. Sen, 'MicroRNA as Biomarkers and Diagnostics', *J. Cell. Physiol.*, vol. 231, no. 1, pp. 25–30, Jan. 2016, doi: 10.1002/JCP.25056.

[4] J. Y. H. Chang and S. Ladame, *Diagnostic, prognostic, and predictive biomarkers for cancer*. Elsevier Ltd., 2019.

[5] L. Petrou and S. Ladame, 'On-chip miRNA extraction platforms: Recent technological advances and implications for next generation point-of-care nucleic acid tests', *R. Soc. Chem.*, vol. 22, no. 3, pp. 463–475, 2022, doi: 10.1039/d1lc00868d.

[6] R. W. Carthew and E. J. Sontheimer, 'Origins and Mechanisms of miRNAs and siRNAs', *Cell*, vol. 136, no. 4, pp. 642–655, Feb. 2009, doi: 10.1016/J.CELL.2009.01.035.

[7] J. A. Weber *et al.*, 'The microRNA spectrum in 12 body fluids', *Clin. Chem.*, vol. 56, no. 11, pp. 1733–1741, 2010, doi: 10.1373/clinchem.2010.147405.

[8] P. S. Mitchell *et al.*, 'Circulating microRNAs as stable blood-based markers for cancer detection', *Proc. Natl. Acad. Sci. U. S. A.*, vol. 105, no. 30, pp. 10513–10518, 2008, doi: 10.1073/pnas.0804549105.

[9] H. H. Cheng *et al.*, 'Plasma Processing Conditions Substantially Influence Circulating microRNA Biomarker Levels', *PLoS One*, vol. 8, no. 6, p. e64795, Jun. 2013, doi: 10.1371/JOURNAL.PONE.0064795.

[10] J. D. Arroyo *et al.*, 'Argonaute2 complexes carry a population of circulating microRNAs independent of vesicles in human plasma', *Proc. Natl. Acad. Sci. U. S. A.*, vol. 108, no. 12, pp. 5003–5008, Mar. 2011, doi: 10.1073/PNAS.1019055108.

[11] A. Turchinovich, L. Weiz, A. Langheinz, and B. Burwinkel, 'Characterization of extracellular circulating microRNA', *Nucleic Acids Res.*, vol. 39, no. 16, pp. 7223–7233, Sep. 2011, doi: 10.1093/NAR/GKR254.

[12] A. Gallo, M. Tandon, I. Alevizos, and G. G. Illei, 'The Majority of MicroRNAs Detectable in Serum and Saliva Is Concentrated in Exosomes', *PLoS One*, vol. 7, no. 3, p. e30679, Mar. 2012, doi: 10.1371/JOURNAL.PONE.0030679.

[13] E. Ban and E. J. Song, 'Considerations and Suggestions for the Reliable Analysis of miRNA in Plasma Using qRT-PCR', *Genes (Basel).*, vol. 13, no. 328, Feb. 2022, doi: 10.3390/GENES13020328.

[14] O. Bryzgunova, M. Konoshenko, I. Zaporozhchenko, A. Yakovlev, and P. Laktionov, 'Isolation of Cell-Free miRNA from Biological Fluids: Influencing Factors and Methods', *Diagnostics 2021, Vol. 11, Page 865*, vol. 11, no. 5, p. 865, May 2021, doi: 10.3390/DIAGNOSTICS11050865.

[15] K. Wright, K. de Silva, A. C. Purdie, and K. M. Plain, 'Comparison of methods for miRNA isolation and quantification from ovine plasma', *Sci. Rep.*, vol. 10, no. 1, p. 825, Dec. 2020, doi: 10.1038/S41598-020-57659-7.

[16] G. Salvi, P. De Los Rios, and M. Vendruscolo, 'Effective interactions between chaotropic

agents and proteins', *Proteins Struct. Funct. Bioinforma.*, vol. 61, no. 3, pp. 492–499, Nov. 2005, doi: 10.1002/PROT.20626.

[17] C. Mitchinson, R. H. Pain, J. R. Vinson, and T. Walker, 'The relative effectiveness of guanidinium and some biguanide slats as denaturants Assessment against penicillinase', *Biochim. Biophys. Acta - Protein Struct. Mol. Enzymol.*, vol. 743, no. 1, pp. 31–36, Feb. 1983, doi: 10.1016/0167-4838(83)90414-4.

[18] D. Guin, K. Sye, K. Dave, and M. Gruebele, 'Dodine as a transparent protein denaturant for circular dichroism and infrared studies', *Protein Soc.*, vol. 25, no. 5, pp. 1061–1068, 2016, doi: 10.1002/pro.2914.

[19] X. Sun, S. Agate, K. S. Salem, L. Lucia, and L. Pal, 'Hydrogel-Based Sensor Networks: Compositions, Properties, and Applications - A Review', *ACS Appl. Bio Mater.*, vol. 4, no. 1, pp. 140–162, Jan. 2021, doi: 10.1021/ACSABM.0C01011/ASSET/IMAGES/MEDIUM/MT0C01011_0008.GIF.

[20] A. Herrmann, R. Haag, and U. Schedler, 'Hydrogels and Their Role in Biosensing Applications', *Adv. Healthc. Mater.*, vol. 10, no. 11, p. 2100062, Jun. 2021, doi: 10.1002/ADHM.202100062.

[21] J. S. Yang, Y. J. Xie, and W. He, 'Research progress on chemical modification of alginate: A review', *Carbohydr. Polym.*, vol. 84, no. 1, pp. 33–39, 2011, doi: 10.1016/j.carbpol.2010.11.048.

[22] P. L. . L. E. . S. F. . K. S. . B. P. . S. L. . M. D. . T. V. . L. S., 'Lateral Flow Test (LFT) Detects Cell-Free MicroRNAs Predictive of Preterm Birth Directly from Human Plasma | Enhanced Reader', *Advanced NanoBiomed Research*, 2022. .

[23] K. Aguilar-Arteaga, J. A. Rodriguez, and E. Barrado, 'Magnetic solids in analytical chemistry: A review', *Anal. Chim. Acta*, vol. 674, no. 2, pp. 157–165, Aug. 2010, doi: 10.1016/J.ACA.2010.06.043.

[24] S. E. Kim, M. Van Tieu, S. Y. Hwang, and M. H. Lee, 'Magnetic particles: Their applications from sample preparations to biosensing platforms', *Micromachines*, vol. 11, no. 3, p. 302, Mar. 2020, doi: 10.3390/MI11030302.

[25] Y. Deng, A. Shavandi, O. V. Okoro, and L. Nie, 'Alginate modification via click chemistry for biomedical applications', *Carbohydr. Polym.*, vol. 270, p. 118360, Oct. 2021, doi: 10.1016/J.CARBPOL.2021.118360.

[26] D. P. Nair *et al.*, 'The Thiol-Michael addition click reaction: A powerful and widely used tool in materials chemistry', *Chem. Mater.*, vol. 26, no. 1, pp. 724–744, Jan. 2014, doi: 10.1021/CM402180T/ASSET/IMAGES/LARGE/CM-2013-02180T_0024.JPEG.

[27] M. C. Nielsen and T. Ulven, 'Selective extraction of G-quadruplex ligands from a rationally designed scaffold-based dynamic combinatorial library', *Chem. - A Eur. J.*, vol. 14, no. 31, pp. 9487–9490, Oct. 2008, doi: 10.1002/CHEM.200801109.

[28] Y. Oki *et al.*, 'Switching of Cell Proliferation/Differentiation in Thiol-Maleimide Clickable Microcapsules Triggered by in Situ Conjugation of Biomimetic Peptides', *Biomacromolecules*, vol. 20, no. 6, pp. 2350–2359, 2019, doi: 10.1021/acs.biomac.9b00333.

[29] S. J. Bryant, K. A. Davis-Arehart, N. Luo, R. K. Shoemaker, J. A. Arthur, and K. S. Anseth, 'Synthesis and characterization of photopolymerized multifunctional hydrogels: Water-soluble poly(vinyl alcohol) and chondroitin sulfate macromers for chondrocyte encapsulation', *Macromolecules*, vol. 37, no. 18, pp. 6726–6733, Jul. 2004, doi: 10.1021/MA0499324/ASSET/IMAGES/LARGE/MA0499324F00007.JPEG.

[30] E. A. Growney Kalaf, R. Flores, J. G. Bledsoe, and S. A. Sell, 'Characterization of slow-gelling alginate hydrogels for intervertebral disc tissue-engineering applications', *Mater. Sci. Eng. C*, vol. 63, pp. 198–210, 2016, doi: 10.1016/j.msec.2016.02.067.

[31] X. Meng, G. Yang, F. Li, T. Liang, W. Lai, and H. Xu, 'Sensitive Detection of Staphylococcus aureus with Vancomycin-Conjugated Magnetic Beads as Enrichment Carriers Combined with Flow Cytometry', *ACS Appl. Mater. Interfaces*, vol. 9, no. 25, pp. 21464–21472, Jun. 2017, doi: 10.1021/ACSAMI.7B05479.

[32] D. M. Togashi, A. G. Ryder, and D. O'Shaughnessy, 'Monitoring local unfolding of bovine

serum albumin during denaturation using steady-state and time-resolved fluorescence spectroscopy', *J. Fluoresc.*, vol. 20, no. 2, pp. 441–452, Mar. 2010, doi: 10.1007/S10895-009-0566-8.

[33] O. Teenan *et al.*, 'Sonoporation of Human Renal Proximal Tubular Epithelial Cells In Vitro to Enhance the Liberation of Intracellular miRNA Biomarkers', *Ultrasound Med. Biol.*, vol. 48, no. 6, pp. 1019–1032, Jun. 2022, doi: 10.1016/J.ULTRASMEDBIO.2022.01.019.

[34] O. K. Gasymov and B. J. Glasgow, 'ANS fluorescence: potential to augment the identification of the external binding sites of proteins', *Biochim. Biophys. Acta*, vol. 1774, no. 3, pp. 403–411, Mar. 2007, doi: 10.1016/J.BBAPAP.2007.01.002.

[35] S. Kelly; N. Price, 'The application of circular dichroism to studies of protein folding and unfolding', *Biochim. Biophys. Acta*, vol. 1338, pp. 161–185, 1997, doi: 10.1016/s0167-4838(96)00190-2.

[36] M. Franzreb, M. Siemann-Herzberg, T. J. Hobley, and O. R. T. Thomas, 'Protein purification using magnetic adsorbent particles', *Appl. Microbiol. Biotechnol.*, vol. 70, no. 5, pp. 505–516, Feb. 2006, doi: 10.1007/S00253-006-0344-3/TABLES/4.

[37] I. Gessner *et al.*, 'Selective Capture and Purification of MicroRNAs and Intracellular Proteins through Antisense-vectorized Magnetic Nanobeads', *Sci. Reports 2019 91*, vol. 9, no. 1, pp. 1–10, Feb. 2019, doi: 10.1038/s41598-019-39575-7.

[38] S. Bhattacharjee, 'DLS and zeta potential – What they are and what they are not?', *J. Control. Release*, vol. 235, pp. 337–351, Jun. 2016, doi: 10.1016/J.JCONREL.2016.06.017.

[39] B. A. Caine, C. Dardonville, and P. L. A. Popelier, 'Prediction of Aqueous pKa Values for Guanidine-Containing Compounds Using Ab Initio Gas-Phase Equilibrium Bond Lengths', *ACS Omega*, vol. 3, no. 4, pp. 3835–3850, Apr. 2018, doi: 10.1021/ACSOMEGA.8B00142/ASSET/IMAGES/MEDIUM/AO-2018-00142U_0007.GIF.

[40] J. N. Scott, N. V. Nucci, and J. M. Vanderkooi, 'Changes in Water Structure Induced by the Guanidinium Cation and Implications for Protein Denaturation', *J. Phys. Chem. A*, vol. 112, no. 43, pp. 10939–10948, Oct. 2008, doi: 10.1021/JP8058239.

[41] K. Wallevik, 'Reversible denaturation of human serum albumin by pH, temperature, and guanidine hydrochloride followed by optical rotation.', *J. Biol. Chem.*, vol. 248, no. 8, pp. 2650–2655, 1973, doi: 10.1016/s0021-9258(19)44056-8.

[42] K. Weber and D. J. Kuter, 'Reversible denaturation of enzymes by sodium dodecyl sulfate.', *J. Biol. Chem.*, vol. 246, no. 14, pp. 4504–4509, 1971, doi: 10.1016/s0021-9258(18)62040-x.

[43] A. E. Jenike and M. K. Halushka, 'miR-21: a non-specific biomarker of all maladies', *Biomark. Res.*, vol. 9, no. 18, pp. 1–7, Dec. 2021, doi: 10.1186/S40364-021-00272-1/TABLES/2.

[44] P. Kralik and M. Ricchi, 'A basic guide to real time PCR in microbial diagnostics: Definitions, parameters, and everything', *Front. Microbiol.*, vol. 8, no. 108, p. 108, Feb. 2017, doi: 10.3389/FMICB.2017.00108/BIBTEX.

[45] F. Balzano *et al.*, 'miRNA Stability in Frozen Plasma Samples', *Molecules*, vol. 20, no. 10, pp. 19030–19040, Oct. 2015, doi: 10.3390/MOLECULES201019030.

I.

APPENDIX

a)

b)

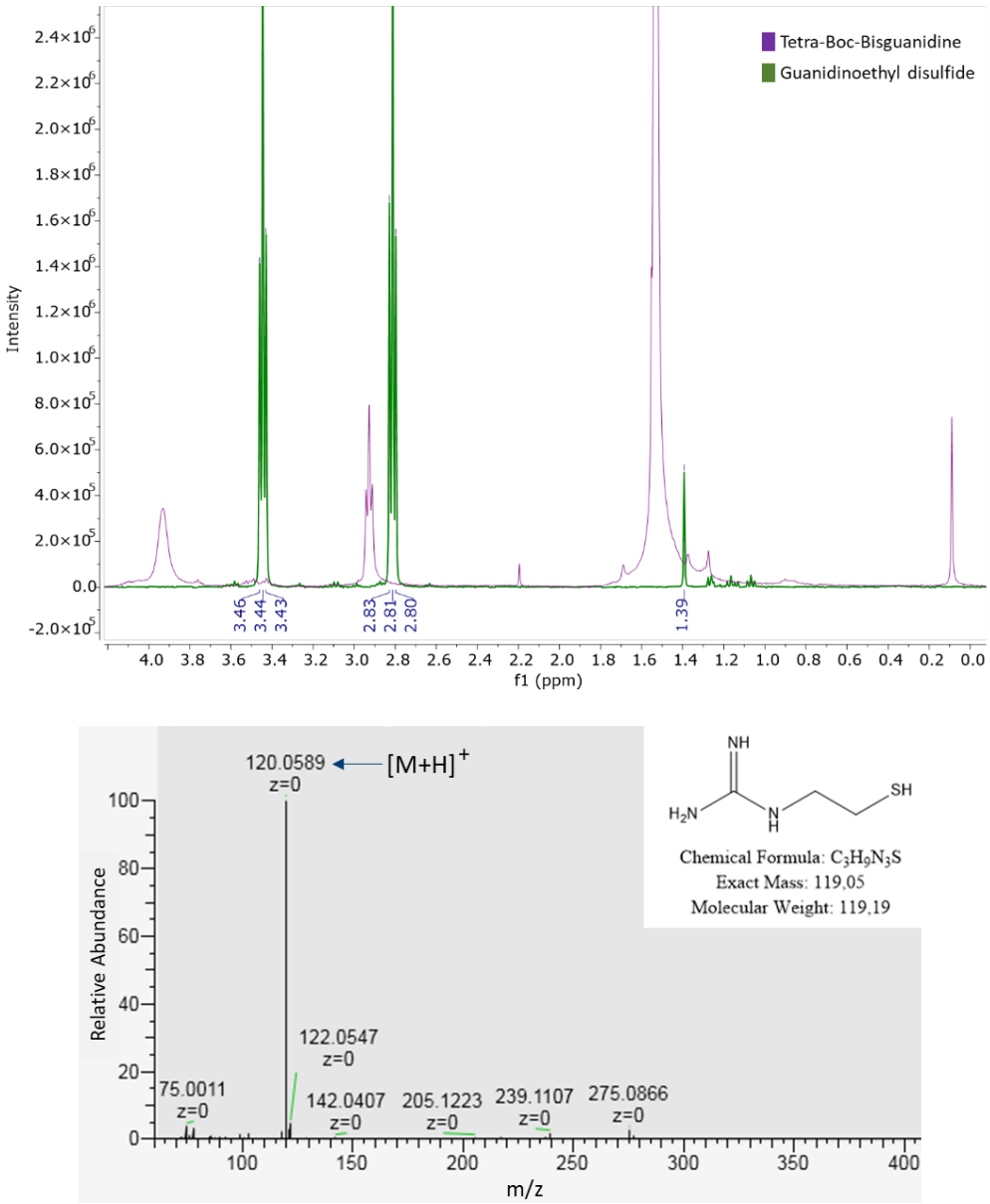

Figure I.1 a) 1H-NMR spectra of tetra-boc-bisguanidine and guanidinoethyl disulfide (^{1}H-NMR (D_2O, 400 MHz): 3.54 (t, J = 6.2 Hz, 4H), 2.91 (t, J = 6.3 Hz, 4H), 1.50 (s, 36H).); b) LC-MS of the guanidinoethyl purified.

a)

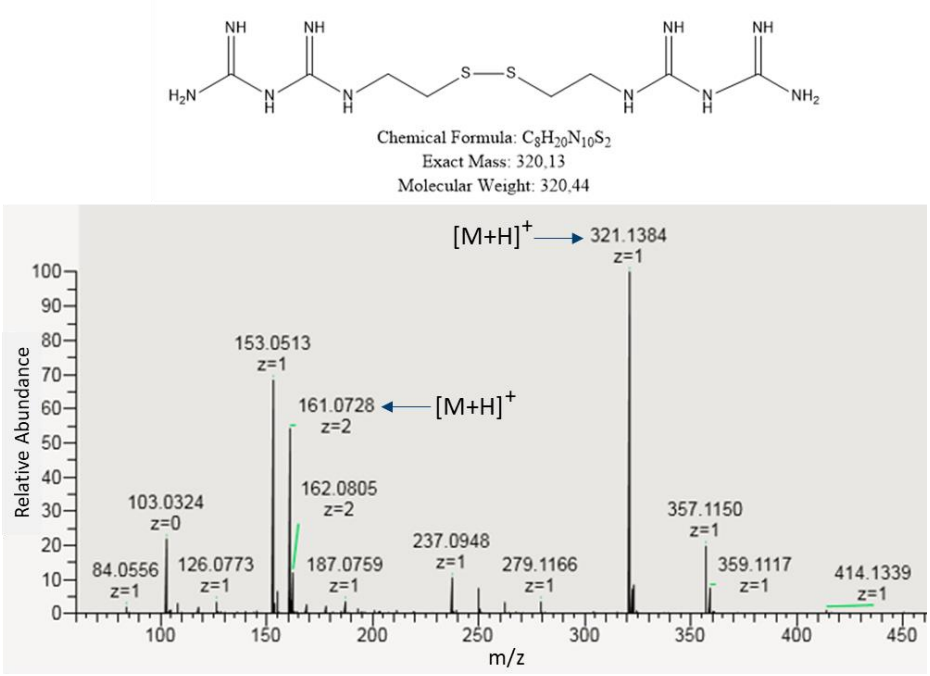

b)

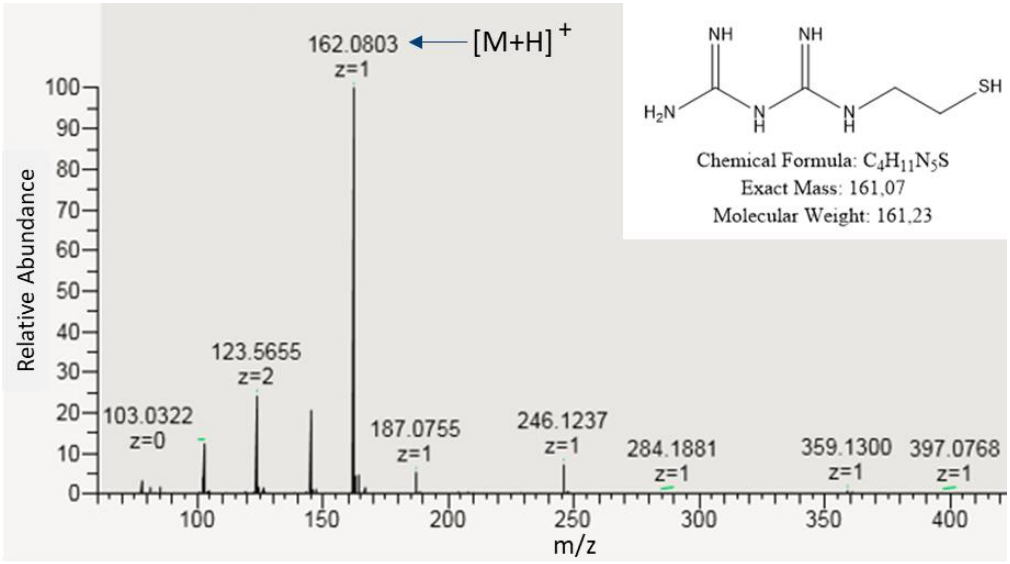

Figure I.2 LC-MS spectra of a) bisguanidinium disulfide and b) bisguanidinium purified.

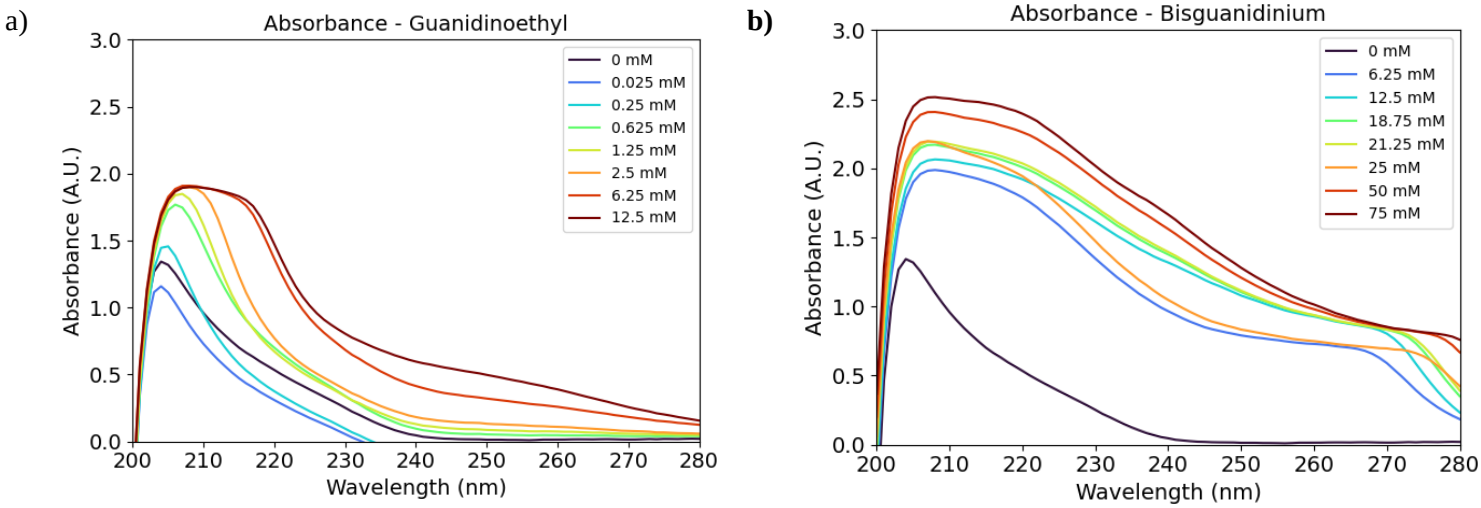

Figure I.3 Absorbance spectrum a) guanidinoethyl and b) bisguanidinium.

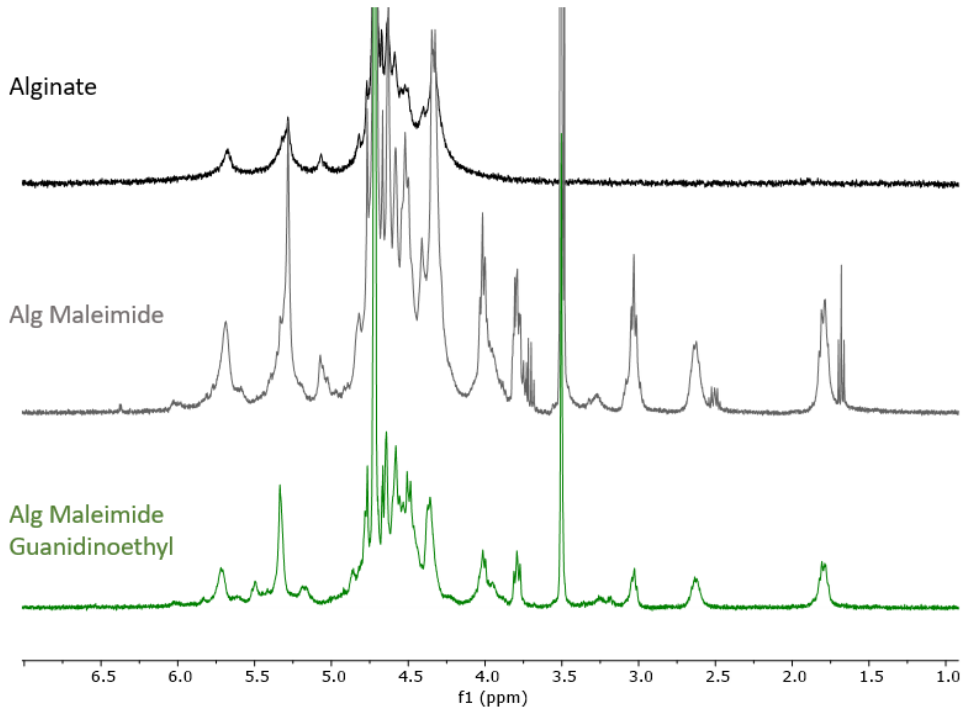

Figure I.4 ^{1}H NMR spectra (D_2O, 400 MHz) of the alginate (black line); alginate functionalized with maleimide (grey line, maleimide chemical shift at 6.2 ppm) and alginate further functionalized with guanidinoethyl (green line).

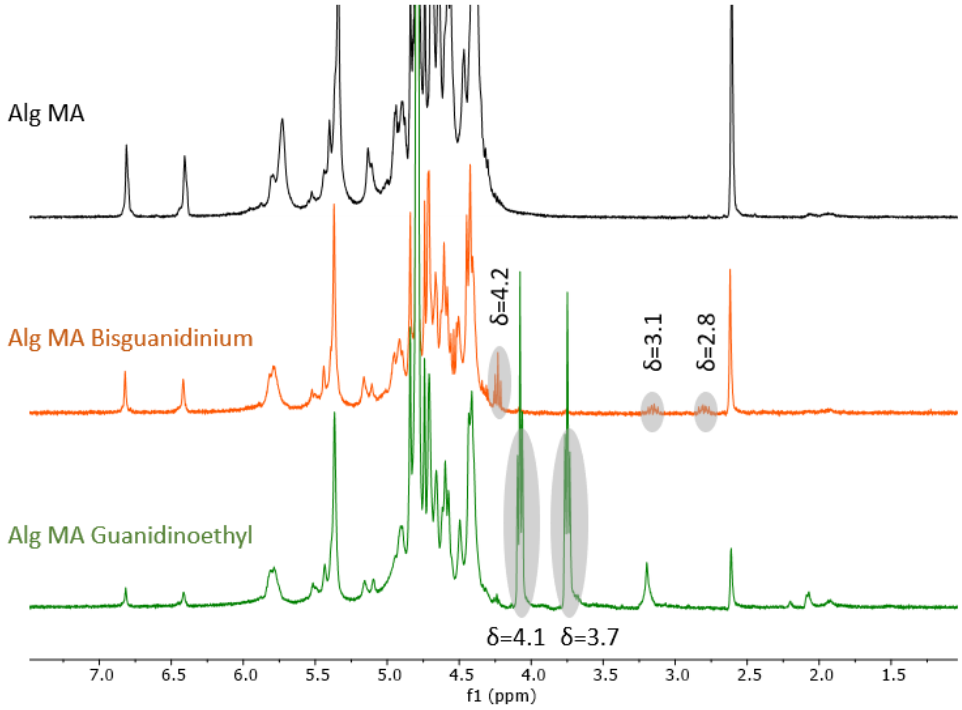

Figure I.5 ^{1}H NMR spectra (D_2O, 400 MHz) of the commercial Alg MA (black line); Alg MA functionalized with bisguanidinium (orange line) or with guanidinoethyl (green line). Grey ovals highlight the coupled molecules.

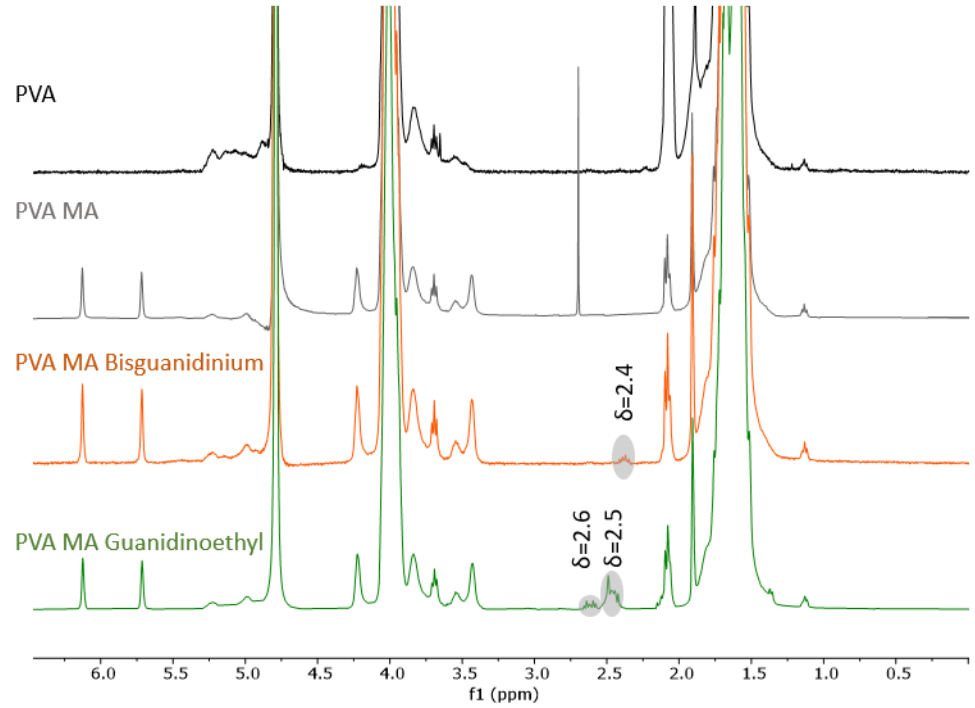

Figure I.6 ^{1}H NMR spectra (D_2O, 400 MHz) of the PVA (black line); PVA MA (grey line); PVA MA functionalized with bisguanidinium (orange line) or with guanidinoethyl (green line). Grey ovals highlight the coupled molecules.

2022

JOANA MIRANDA SALREU MARTINHO

ENGINEERING AND CHARACTERIZATION OF NOVEL DENATURING PLATFORMS FOR AUTOMATED RELEASE OF miRNAS FROM CARRIER PROTEINS AND EXOSOMES

NOVA SCHOOL OF SCIENCE & TECHNOLOGY